Experimental Study of Time-averaged Flow and Turbulence over Asymmetric Tidal Dunes

Kevin Bobiles[1,2], Bernhard Kondziella[3], Christina Carstensen[3,4], Elda Miramontes[1,2], Ingrid Holzwarth[3] and Alice Lefebvre[1]

[1]MARUM – Center for Marine Environmental Sciences, University of Bremen, Bremen, Germany
[2]Faculty of Geosciences, University of Bremen, Bremen, Germany
[3]Federal Waterways Engineering and Research Institute (BAW), Hamburg, Germany
[4]Present address: Federal Waterways and Shipping Administration (WSV), Kiel, Germany

Correspondence to: Kevin Bobiles (kbobiles@marum.de)

Abstract. Asymmetric tidal dunes with intermediate (10-17°) to low-angle slopes (< 10°), usually with an irregularly-shaped lee side, are often found in natural, constrained tidal environments such as tidal rivers, estuaries and tidal channels. However, previous studies on bedform flow dynamics have largely focused on high-angle dunes with a simple (straight) lee side, generally found in flume studies or small rivers. This study provides a detailed characterisation of the flow and turbulence over asymmetric tidal dunes under an idealised tidal flow condition based on laboratory measurements. Specifically, we aim to address how tidal dune shape, especially the lee side geometry, controls the properties of flow separation and resulting turbulence structures. Furthermore, we address how flow bidirectionality changes flow and turbulence over the same tidal dune geometry. To achieve this, we conducted large-scale, high-resolution flume experiments over two idealised dune morphologies which represent natural asymmetric tidal dunes with intermediate- to low-angle slopes. The flow condition was an idealised representation of tidal flow for which the same unidirectional steady currents were imposed first in one direction, then in the opposite direction. Our results show that for the case of an intermediate-angle tidal dune and when the flow was directed from the gentle stoss to the steep lee slope, a downward expanding turbulent wake and a small, near-bed permanent flow separation were detected. A small flow separation was also detected for the case of low-angle tidal dune. When the flow was reversed and directed from the steep stoss to the gentle lee slope, flow direction significantly altered the flow dynamics for both dunes as no permanent flow separation was observed and turbulence structure was similar to that over a flat bed. Interestingly, we demonstrated that a small intermittent flow separation can still form even for tidal dunes with very gentle slope (4°) provided that a short steep portion is present. This implies that low-angle dunes can generate flow resistance and can potentially contribute to sediment mobilisation above low-angle dunes. Overall, our study highlights the significant impact of dune morphology, particularly the lee side slopes, and flow direction on the flow and turbulence dynamics above asymmetric tidal dunes. Our findings can have further implications on the parameterisation of hydraulic roughness, estimation of sediment transport and the resulting morphodynamics in natural shallow water environments.

1 Introduction

The coastal environment is a highly dynamic and active portion of the Earth's surface where the ocean meets the land. Under the action of river, tidal, wind and wave-driven currents, sediments can be mobilised and frequently form both small- and large-scale rhythmic undulations, collectively known as bedforms (Dalrymple and Rhodes, 1995). Among these, dunes are large (decimeters to meters in height, meters to hundreds of meters in length) bedforms which are particularly abundant in lower reaches of rivers (Lange et al., 2008; Cisneros et al., 2020), estuaries (Aliotta and Perillo, 1987; Bradley et al., 2013; De Lange et al., 2024) and in coastal tidal environments (Damen et al., 2018), where they develop into large fields with complex morphologies. Despite their prevalence in natural flow environments, the detailed characteristics of flow and turbulence structures over intermediate- to low-angle tidal dunes under unsteady, reversing tidal flows remain poorly studied, even though such conditions dominate many estuaries and tidal rivers. It is necessary to address this knowledge gap in dune flow dynamics since dunes are one of the drivers of flow resistance and sediment transport in tidal rivers and coastal estuarine environments (Best, 2005; Coleman and Nikora, 2011; Venditti, 2013; De Lange et al., 2021). Resolving dune-induced flow and turbulence under tidal forcing is essential for understanding hydro-morphodynamic feedbacks (Villard and Kostaschuk, 1998; Kostaschuk et al., 2004; Herrling et al., 2021) and for various applications such as navigation and waterway management (Nasner et al., 2009) as well as subsea cable burial and offshore construction.

Insights on dune morphology are crucial in the understanding of the flow and turbulence dynamics. Depending on their morphology, dunes can be classified as angle-of-repose, high-, intermediate- or low-angle dunes based on their mean lee slopes (Lefebvre and Cisneros, 2023) (Fig. 1). Angle-of-repose (slope > 24°) and high-angle dunes (slope > 17°) have heights usually on the order of 1/6 of the water depth (Bradley and Venditti, 2017) and are commonly found in small rivers and laboratory flumes (Venditti et al., 2005; Naqshband et al., 2014) where a unidirectional current is the dominant flow condition. Intermediate dunes have lee slopes between ca. 10° and 17° and are often found in large rivers (Cisneros et al., 2022). Low-angle dunes with lee slopes of less than 10° are mostly found in large tidal rivers, estuaries and tide-dominated shelves (Nasner, 1974; Aliotta and Perillo, 1987; Lefebvre et al., 2021). Importantly, however, these associations between dune lee slopes, environment type and main flow forcing should be viewed as trends rather than strict classification because dune classification reflects the combined influences of several factors such as dune morphology, environment, hydrodynamics, sedimentology and migration dynamics to name a few.

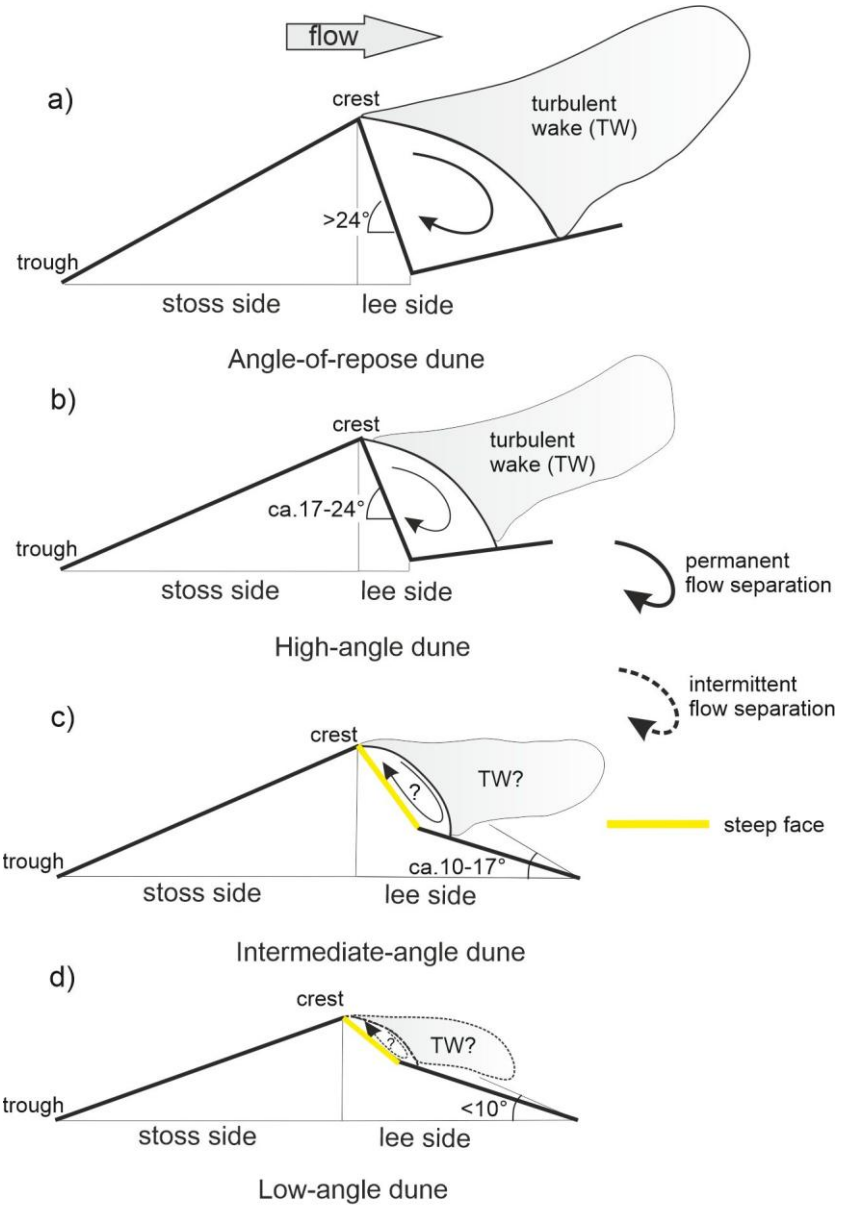

Figure 1: Types of dunes based on their morphology. TW: Turbulent wake.

Dune morphology influence the flow and turbulence structures primarily through the lee side geometry (Kwoll et al., 2016). In particular, the steep face, which is the lee side slope downstream of the crest that is steeper than the mean lee slope and its adjacent segments, strongly governs whether flow separation is permanent, intermittent or absent. When flow separation forms,

the steep face controls the shape, extent and intensity of the flow separation and the resulting turbulent wake (Fig. 1) (Lefebvre et al., 2016; Lefebvre and Cisneros, 2023). The overall characteristics of the mean flow and turbulence structures over angle-of-repose dunes are already well documented (Nelson et al., 1993; Mclean et al., 1994; Bennett and Best, 1995; Venditti and Bennett, 2000; Best, 2005; Lefebvre et al., 2014). Above angle-of-repose dunes (Fig. 1a), flow accelerates over the stoss side until it reaches the crest and decelerates over the lee side forming a permanent flow separation zone where a reverse flow is observed. A shear layer, which separates the flow recirculation cell from the overlying undisturbed flow, forms and expands. Kelvin-Helmholtz instabilities develop along this separated shear layer where strong velocity gradient become unstable, generating periodic roll-up and shedding of vortices that give rise to a large turbulent wake. This turbulent wake expands upward and advects over the stoss side of the adjacent dune. Below this turbulent wake, a newly formed internal boundary layer develops, with a logarithmic velocity profile. Because of the resulting flow structure, a maximum horizontal velocity located at the crest develops and is expected to generate high bottom shear stress capable of generating bedload and suspended sediment transports contributing to the morphodynamic changes of bottom topography. Over high-angle dunes (Fig. 1b), a flow separation and turbulent wake are found, but their size and intensity are reduced compared to those above angle-of-repose dunes (Lefebvre and Cisneros, 2023; Kwoll et al., 2016; Kwoll et al., 2017).

Intermediate-angle dunes (Fig. 1c) rarely have a permanent flow separation but are likely to possess an intermittent flow separation (Kostaschuk and Villard, 1996; Roden, 1998; Best and Kostaschuk, 2002; Sukhodolov et al., 2006; Lefebvre and Cisneros, 2023). Turbulence is weaker than over high-angle dunes, but will usually display a distinct wake above the trough (Lefebvre and Cisneros, 2023). For low-angle dunes (Fig. 1d), several studies report the absence of permanent flow separation and some intermittent flow separation may be present (Kostaschuk and Villard, 1996; Roden, 1998; Carling et al., 2000; Best and Kostaschuk, 2002; Sukhodolov et al., 2006; Kwoll et al., 2016). Turbulence over low-angle dunes is expected to be weaker than that of high-angle dunes and might be even similar to that over a flatbed condition (Kline et al., 1967). While these earlier findings highlight the importance of lee side geometry, the conditions under which flow separation transitions between nonexistent, intermittent and permanent separation and how these transitions reorganise turbulence are still not fully resolved for intermediate to low-angle dunes.

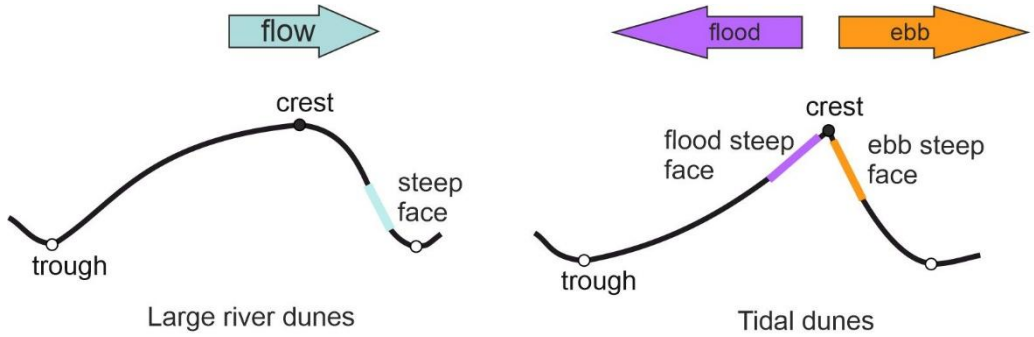

Figure 2: Schematic representations of river and tidal dunes.

In addition to the lee side geometry, the overall morphology of river and tidal dunes exhibits contrasting shapes (Fig. 2) and is also thought to control flow separation, turbulence and therefore the associated hydraulic form roughness. Low-angle river dunes often have rounded crests with the steepest lee slope located closer to the trough (Lefebvre et al., 2016; Cisneros et al., 2020), whereas low-angle tidal dunes tend to have sharper crests with the steepest segment positioned nearer the crest (Dalrymple and Rhodes, 1995; Lefebvre et al., 2021). In tidal settings, not only the bedform crest shape, but also the reversing of the tidal currents have an influence on the interaction between dune and flow. Most laboratory and numerical studies have focused on steady unidirectional currents whereas realistic tidal environments impose systematic flow reversal and evolving flow intensity over a tidal cycle. Recent flume experiments further emphasized the need to elucidate flow dynamics over estuarine and tidal dunes under conditions that better approximate tidal forcing (Carstensen and Holzwarth, 2023; Porcile et al., 2025). Flow bidirectionality changes which dune side acts as the effective lee side, potentially suppressing flow separation, modifying shear layer development, effective hydraulic roughness (Herrling et al., 2021; De Lange et al., 2021; De Lange et al., 2024) and reorganising turbulent events that drive momentum exchange and sediment suspension.

The present study addresses the following research questions. How do intermediate and low-angle tidal dune morphologies, specifically the mean lee slopes and steep face, control the presence and structure of flow separation and resulting turbulence? And how does flow bidirectionality, representative of natural ebb-flood flow reversals, reorganise flow separation and the associated turbulence structures over the same fixed dune geometry? By addressing these questions, we aim to bridge the gaps on the understanding of flow and turbulence dynamics between angle-of-repose to high-angle dunes and intermediate- to low-angle dunes. Furthermore, we want to characterise the influence of bidirectionality on flow over dunes and, hence, provide elements of a realistic representation of flow over natural tidal dunes.

To answer these questions, we conduct high-resolution, large-scale flume experiments to measure time-averaged flow and turbulence above representative two-dimensional fixed tidal dune fields under idealised bidirectional flows. The laboratory

dunes cover the intermediate- to low-angle configurations (< 17°) with segmented lee sides and steepest slopes positioned near the crest, consistent with tidal dune morphology (Fig. 2). The chosen slopes cover the expected transition from nonexistent to intermittent to permanent flow separation. The large-scale nature of our flume experiments enables robust measurements in the near bottom region of the flow and the imposed bidirectionality provides controlled insight into how flow reversal modifies dune-induced flow separation and turbulence. We first proceed by describing the experimental methodology of our flume experiments and our laboratory dunes. We then present the time-averaged flow field and other derived flow and turbulence structures for each dune and flow configuration. We proceed further with the interpretation of how dune morphology and flow bidirectionality interact in shaping the observed flow dynamics. Finally, we discuss some implications for realistic tidal dune dynamics and sediment transport processes and summarizes the key findings in this study.

2 Experimental methodology

2.1 Experimental facility

Laboratory experiments were conducted in the large recirculating flume of the Federal Waterways Engineering and Research Institute in Hamburg (Bundesanstalt für Wasserbau, BAW Hamburg). The recirculating flume has an overall length of 220 m consisting of two straight sections connected by a semi-circular segment at both ends (Fig. 3). The straight channel section has a length of 70 m, a width of 1.5 m and a maximum water depth of 1.3 m. The flow is generated by a bow thruster pump located in an underground pipeline at the opposite side of the straight channel section. A maximum flow velocity of 1 m/s can be imposed in either direction by reversing the pump flow direction. Carstensen and Holzwarth (2023) showed that secondary flows at both ends of the straight channel section can be attributed to geometric configurations such as bends or curves in the channel and to fluctuating turbulence associated with the pump generation itself. In order to avoid the influence of secondary flows, measurements were taken far away (around 30 m) from the bends (Fig. 3).

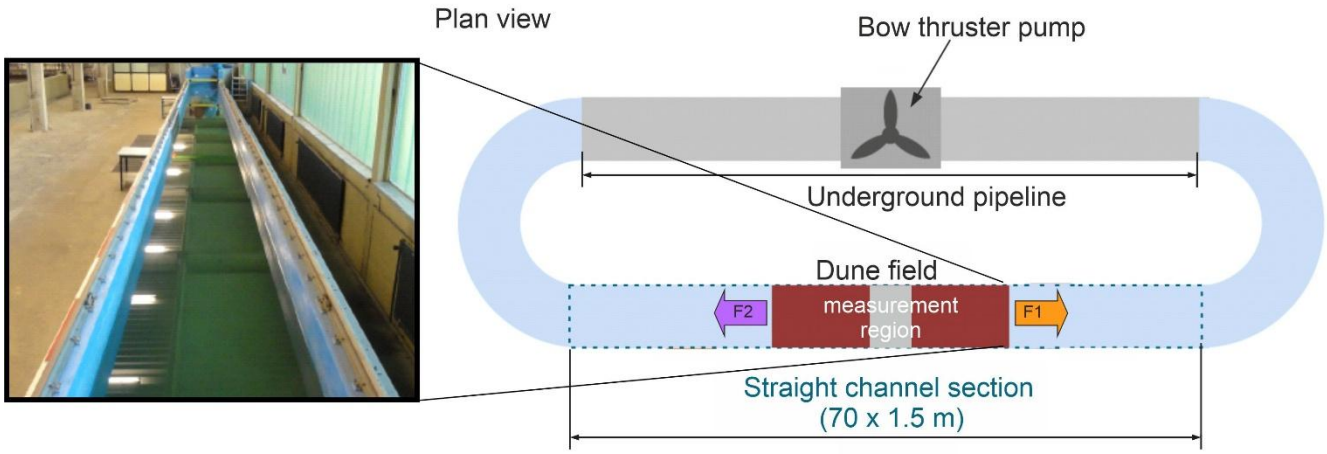

Figure 3: Schematic diagram of the recirculating flume.

2.2 Modelled tidal dunes and hydrodynamic conditions

The shapes and dimensions of the laboratory dunes are depicted in Fig. 4 and their morphological properties are summarised in Table 1. The dunes used in this study were modelled following the dunes found in the tidal river part of the Weser, upstream from the estuarine part, in a region without salt water but influenced by tidal currents (Lefebvre et al., 2021). The dimensions and slopes of the field tidal dunes are summarised in Table 1. Intermediate angle field dunes with maximum steep side angle of 22.5° and mean steep side angle of 12° account for 10% of the observed dunes in the Weser. These dunes are expected to generate considerable turbulence and, thus, have a strong influence on flow resistance. Low angle field dunes with maximum steep side angle of 14.2° and mean steep side angle of 8.5° are the dominant type of dune (48%) observed in the Weser. These dunes are only expected to generate intermittent flow separation and turbulence with intensities proportional to the slope of the steep face. The laboratory dunes are obtained by applying a Froude scaling with a length scale of 1:15. Specifically, laboratory dune 1 is an idealised representation of an intermediate-angle tidal dune and laboratory dune 2 is an idealised representation of a low-angle tidal dune. Both laboratory dunes maintained a constant bedform height to water depth ratio (H/h) of 0.15 and bedform aspect ratio (H/L) of 0.05 consistent with previous observations (Bennett and Best, 1995; Bradley and Venditti, 2017). These nondimensional parameters ensure that the generated velocity field is representative of the flow above fully developed bedforms.

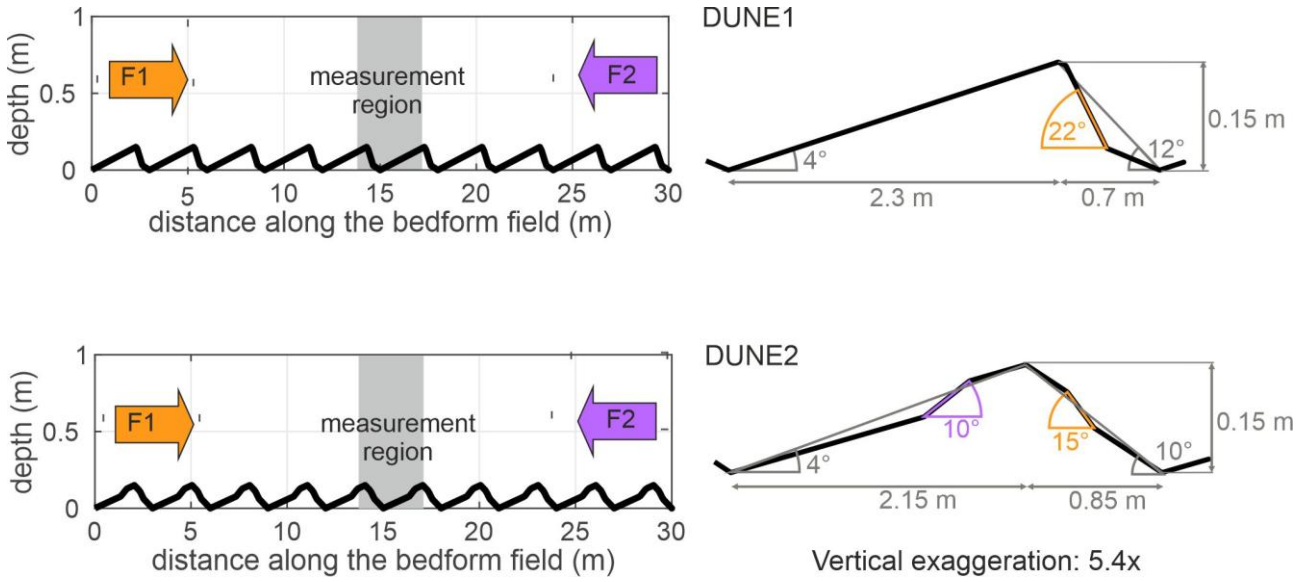

Figure 4. Laboratory tidal dunes and experimental flume setup.

The relevant morphological parameters of a tidal dune are depicted in Fig. 5. F1 and F2 represent ebb and flood flows, respectively. H is the bedform height defined as the vertical distance from the trough to the crest and L is the bedform length defined as the horizontal distance between either crest or troughs of adjacent dunes. The steep side is the side of the dune where the flow is aligned with the dune asymmetry (i.e., F1 flow). The gentle side, on the other hand, is the side of the dune where the flow opposes the dune asymmetry (i.e., F2 flow). We refer to "flow aligned with the dune asymmetry" when the flow is going over the steeper side of the dune and "flow opposed the dune asymmetry" when the flow is going over the gentler side of the dune. The corresponding mean and maximum angles are also shown in Fig. 5. Steep face height, H_{SF}, is defined as the vertical projection of the steep face.

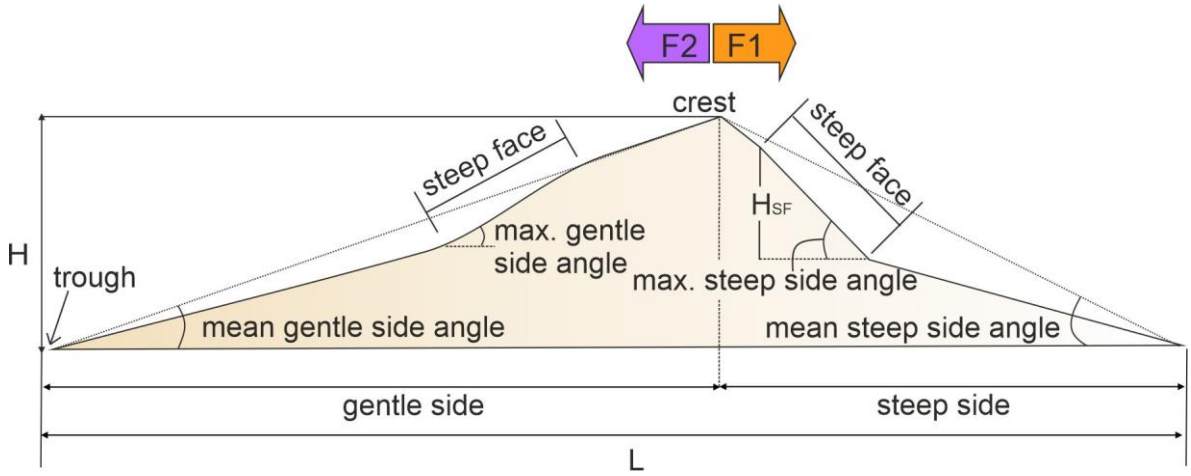

Figure 5. Schematic diagram of tidal dune morphology. H is the bedform height, H_{SF} is the steep face height, L is the bedform length, F1 refers to the flow that is aligned with the dune asymmetry (i.e., the flow is directed from the gentle stoss to the steep lee slope) and F2 refers to the flow that is opposing the dune asymmetry (i.e., the flow is directed from the steep stoss to the gentle lee slope).

The hydrodynamic conditions such as water levels, flow velocities and flow directions in the Weser Estuary change during every ebb-flood and spring-neap tidal cycle and, thus, flow velocity and water levels vary following various cycles (Lange et al., 2008; Lefebvre et al., 2021). Since our flume experiments are not intended to reproduce the full tidal conditions in the Weser, this study simply adopts representative flow conditions that are comparable to the field conditions. Steady currents, defined as F1 and F2 depth-averaged flow velocities, are imposed first in one, then in another direction, with a magnitude of 0.3 m/s. The mean water depth is set to 1.0 m. These scaled down conditions are based on the maximum flow velocity during ebb phase at the Weser which is about 1.0 m/s and the mean water depth is about 14 m at the area of Weser where intermediate to low-angle dunes are observed (Lefebvre et al., 2021; Carstensen and Holzwarth, 2023). The flow conditions at the laboratory are scaled down through Froude scaling based from the observed hydrodynamic conditions at the Weser. The Froude number which is the ratio of the inertial force to the restoring gravitational force ($Fr = U/\sqrt{(gh)}$) provides the relative importance of inertial forces acting on fluid particles to the weight of the particle. The Froude number is a widely used parameter in scaling down field to laboratory properties involving free surface flow. The resulting Froude number is the same for both scales implying dynamic similarity between field and laboratory dunes. The hydrodynamic conditions at both field and laboratory scales are also summarised in Table 1.

2.3 Experimental setup

The two laboratory dunes and the setup inside the recirculating flume are shown in Fig. 4. The fixed dunes were made from concrete and were fine-sandblasted to provide a natural grain roughness. Measurements were conducted in two opposite flow directions (i.e., F1 and F2 flows) for the two laboratory dunes. For each measurement, the mean water depth, dune length,

dune height and flow velocity were kept constant to allow comparison between measurements. In order to measure flow properties in equilibrium with the dune morphology, a field of 10 identical dunes were deployed at the centreline of the straight channel section of the flume, covering a total distance of 30 m, and measurement region for each flow direction was above the 5th dune (Fig. 5).

Table 1. Dune morphology and hydrodynamic conditions between field and laboratory dunes.

Parameters	Intermediate-angle field dunes	Low-angle field dunes	Laboratory dune 1: intermediate-angle	Laboratory dune 2: low-angle
Bedform height (H), m	2.3	1.5	0.15	
Bedform length (L), m	50.9	45.5	3.0	
Bedform aspect ratio (H/L)	0.05	0.04	0.05	
Mean steep side angle (°)	11.9	8.5	12	10
Max. steep side angle (°)	22.5	14.2	22	15
Mean gentle side angle (°)	4.5	3.6	4	4
Max. gentle side angle (°)	10	9	4	10
Mean water depth (h), m	14	13.8	1	
Height-to-depth ratio (H/h)	0.16	0.11	0.15	
Depth-ave. velocity (F1 = F2 = U), m/s	1		0.3	
Froude number	0.08		0.1	
Reynolds number	$1.4 \cdot 10^7$		$3 \cdot 10^5$	

2.4 High-resolution flow measurements

Velocity measurements were conducted using a sideward looking Nortek Acoustic Doppler Velocimeter (ADV), Vectrino (Nortek, 2018). For each flow and dune set up, around 1300-1700 velocity measurements (around 70-90 velocity profiles), each for 2 minutes with a sampling rate of 100 Hz, were conducted (Fig 6). To facilitate quick data acquisition and accurate positioning of the ADV, a motorised metal framed structure (motion unit) was installed on top of the flume, which automatically moved the instrument to a pre-determined location. From here on, we adopt the following conventions for consistency and quick reference to each experimental test. The coordinate axes follow the right-hand rule where positive

horizontal x-axis is pointing to the right, positive horizontal y-axis is pointing inward towards the page and positive vertical z-axis is pointing upward. The velocity components are defined as *u*, *v*, and *w* for x, y and z axes, respectively. 'DUNE1' and 'DUNE2' refer to laboratory dune 1 and laboratory dune 2, respectively (Fig. 5). 'F1' refers to flow condition when the flow is directed from the gentle stoss to the steep lee slope (i.e., flow is aligned with the dune asymmetry) and 'F2' refers to flow condition when the flow is directed from the steep stoss to the gentle lee slope (i.e., flow is opposed to the dune asymmetry). For instance, 'DUNE1_F1' is the test when the flow is aligned with the dune asymmetry above laboratory dune 1.

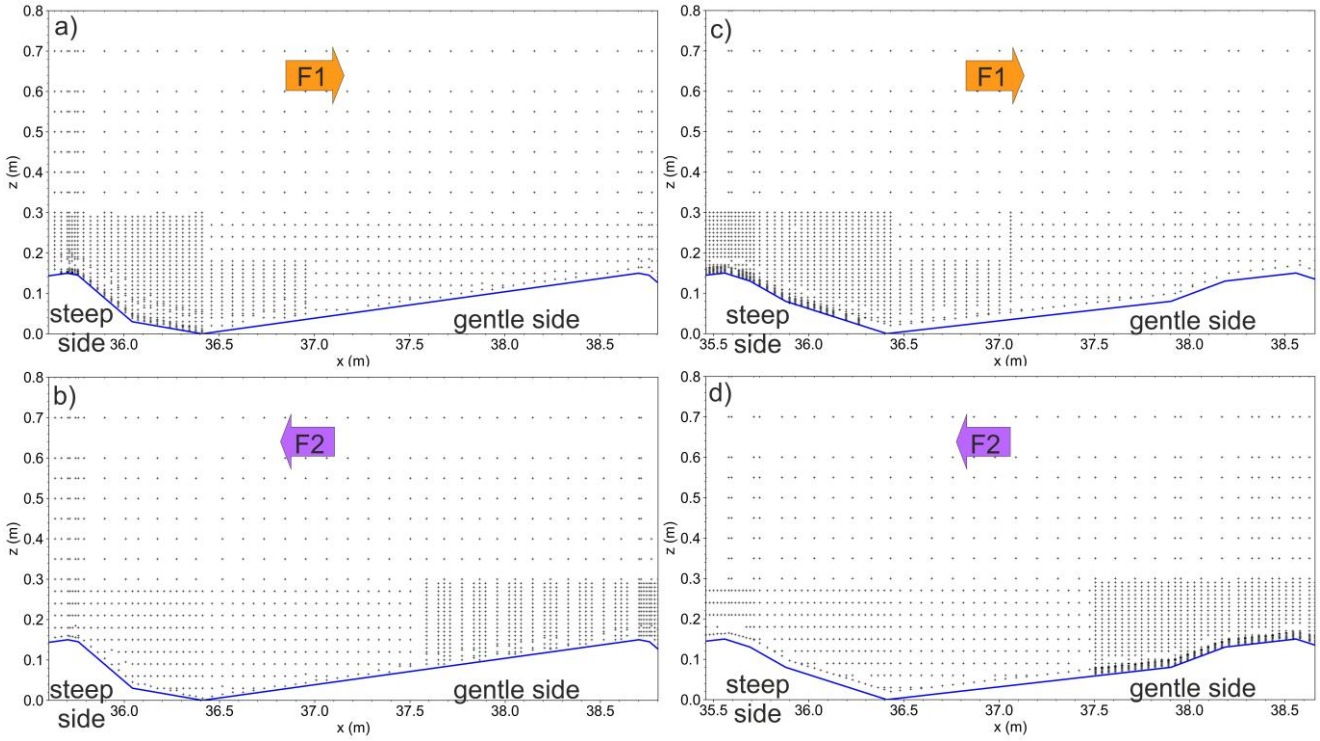

Figure 6. ADV point measurement layout. a) DUNE1_F1, b) DUNE1_F2, c) DUNE2_F1, d) DUNE2_F2. F1: flow aligned with dune asymmetry; F2: flow opposed to dune asymmetry.

2.5 Data processing and analysis

Velocity measurements were processed to generate a high-resolution two-dimensional velocity field and other derived flow and turbulence properties. After despiking the data (Goring and Nikora, 2002), further quality control was performed by inspection of the data signal strength such as the signal-to-noise ratio (SNR) and correlation. Bad quality data not filtered by the above despiking method such as those from multi-reflection coming from the bottom surface were discarded and replaced when their corresponding SNR and correlation were below 15 dB and 80%, respectively. The instantaneous velocities (*u*, *v* and *w*) were separated into their mean and fluctuating components based on Reynolds decomposition. That is, for instantaneous horizontal component u,

$$u = \overline{u} + u' \quad (1)$$

where $\overline{u}$ is the mean (time-averaged) component of the velocity and u' is the fluctuating component of the velocity. The same decomposition can also be done to the *v* and *w* velocity components. The vertical gradient of the mean horizontal velocity, $\partial\overline{u}/\partial z$, is calculated from the mean component of the horizontal velocity, $\overline{u}$.

The intermittency factor, *IF*, which is an indicator of how frequent flow reversal occurs, is calculated from the instantaneous horizontal velocity, u as

$$IF = \frac{N_{reversed\_u}}{N_{total}} \cdot 100 \quad (2)$$

where $N_{reversed\_u}$ is the count in the velocity measurements when the instantaneous horizontal velocity, u, changes its direction from positive to negative flow (i.e., $u < 0$) and N_{total} is the total count of the instantaneous horizontal velocity measurements.

The turbulent kinetic energy (TKE) is calculated from the fluctuating component of each velocity component,

$$TKE = \frac{1}{2}\left(\overline{u'^2} + \overline{v'^2} + \overline{w'^2}\right). \quad (3)$$

A spatially detailed two-dimensional vertical descriptions of the mean flow and turbulence properties are then generated from the ADV point measurements by performing a Kriging interpolation over the entire measurement domain with a 3 mm x 3 mm mesh.

The flow separation line is computed from the velocity profiles as the height above the dune surface where the downstream-directed horizontal volume flux (i.e., flow discharge per unit width) is compensated by the upstream-directed horizontal volume flux (Lefebvre et al., 2014). It is expressed as

$$\int_{z_{dune}}^{z_{FSL}} \overline{u}(z)\, dz = 0, \quad (4)$$

where z_{FSL} and z_{dune} are the elevations of the flow separation line and dune surface measured from zero elevation.

The length of the flow separation zone, $L_{FSZ,}$ is defined as the horizontal distance between the location where the flow separation starts and the point of reattachment. The thickness of the flow separation zone, $Th_{FSZ,}$ is taken as the vertical projection from the dune surface to the flow separation line.

The part of the total shear stress that is associated with turbulence is the Reynolds shear stress, τ_{uw}. The time-averaged Reynolds stress is evaluated based from the velocity fluctuations of the horizontal and vertical components of the velocity and is expressed as

$$\tau_{uw} = -\rho\overline{u'w'}. \quad (5)$$

The Reynolds stress profiles along the entire length of each dune are then further condensed to obtain the spatially-averaged Reynolds stress profiles. The spatially-averaged Reynolds stress profile is determined by averaging an individual Reynolds stress profile along constant elevation about the zero mean bed elevation.

A quadrant analysis is performed to investigate the characteristics of turbulent events by grouping the fluctuating components of the horizontal and vertical components of the velocity (i.e., u' and w') into four quadrants. Quadrant 1 ($+u'$ and $+w'$) is identified as the outward interaction event, quadrant 2 ($-u'$ and $+w'$) as the ejection event, quadrant 3 ($-u'$ and $-w'$) as the wallward interaction event and quadrant 4 ($+u'$ and $-w'$) as the sweep event. Fig. 7 shows a conceptual sketch to visualize the four quadrant events used in characterising the turbulent events. The fluctuating velocity pair can be investigated either through examination of the entire velocity record or only those significant events that lie above a particular pre-defined threshold (*HS* or hole size) which is expressed as

$$HS = \frac{|u'w'|}{u'_{rms}w'_{rms}} \quad (6)$$

where u'_{rms} and w'_{rms} are the root-mean square values of the horizontal and vertical components of the velocity, respectively. Corresponding with previous studies (Bennett and Best, 1995; Best and Kostaschuk, 2002; Kwoll et al., 2016), a hole size (*HS*) of 2 is used to better delineate significant quadrant events from background turbulence, which is especially relevant for quadrants 2 and 4 since they are often classified as positive contributors to Reynolds stress (Bennett and Best, 1995) and sediment transport (Unsworth et al., 2018).

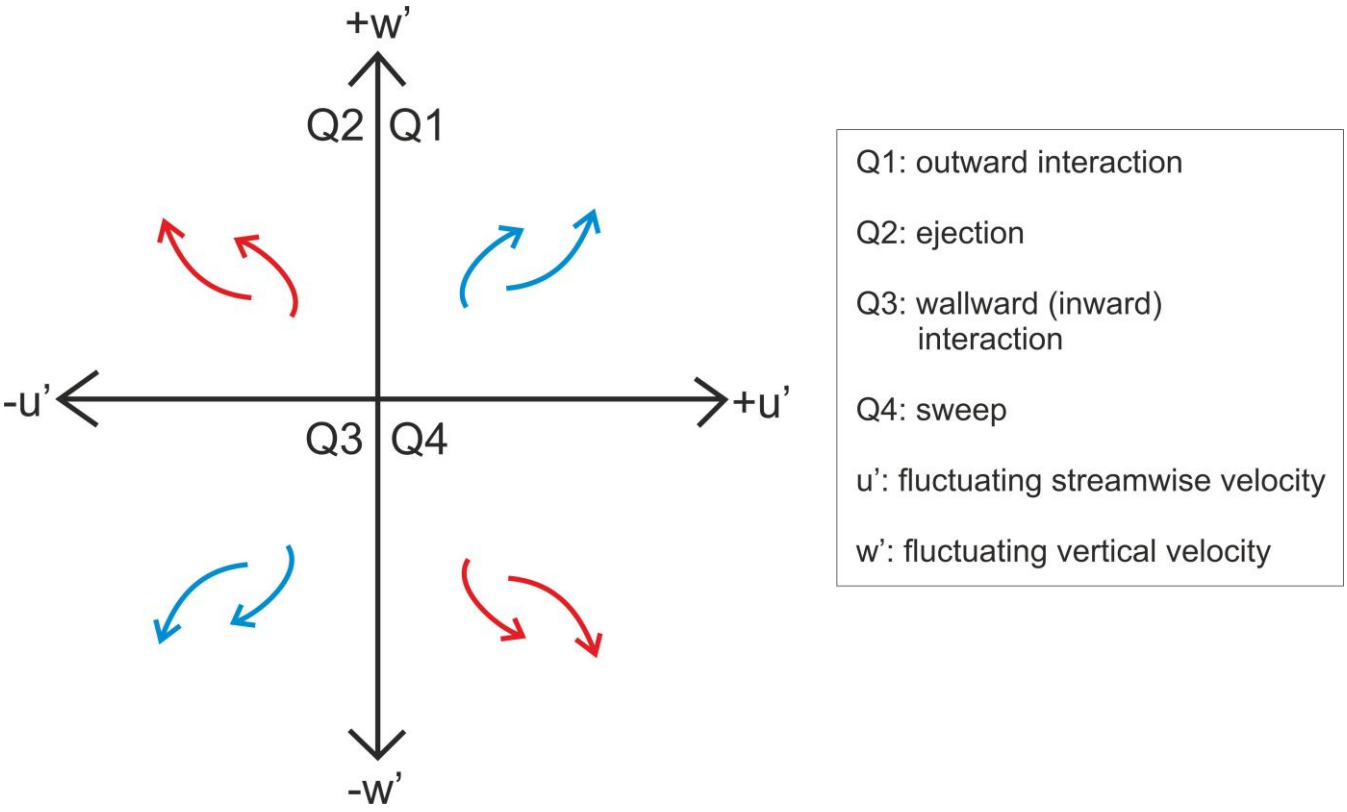

Figure 7. Conceptual diagram showing the different quadrant events used to characterise turbulent events using quadrant analysis.

3 Results

3.1 Characteristics of time-averaged flow over intermediate- and low-angle tidal dunes

The time-averaged flow fields for both dunes with F1 and F2 flow setups are shown in Fig. 8. For DUNE1_F1, a strong deceleration zone characterised by slow mean streamwise velocity and downward directed mean vertical velocity is observed over the steep lee side of the dune. A gradually accelerating flow characterised by the increasing mean streamwise velocity and an upward directed mean vertical velocity is seen above the gentle stoss side of the dune. For DUNE2_F1, the same flow pattern as that of DUNE1_F1 can be observed although its magnitude is decreased especially the mean streamwise velocity.

When the flow is reversed and is now directed from the steep stoss to the gentle lee slope (F2 flow), the acceleration-deceleration flow pattern reverses its occurrence above the dunes. For DUNE1_F2, a weaker deceleration zone compared to that of DUNE1_F1 is observed over the gentle lee side as evident from the gradually decreasing pattern of the mean streamwise velocity. As the stoss side is now steeper than the lee side, a strong upward mean vertical velocity is observed indicating the influence of flow reversal on the mean flow characteristics. The same flow characteristics are observed for DUNE2_F2 with some subtle features due to the presence of short steep section at the gentle lee side. At the location of the short steep section (ca x= 38.0 m), a stronger deceleration zone characterised by slower mean streamwise velocity and stronger downward mean vertical velocity than the rest of the flow structure above the gentle lee slope of the dune is observed. Overall, these observations confirm the influence of topographic forcing on the time-averaged flow fields.

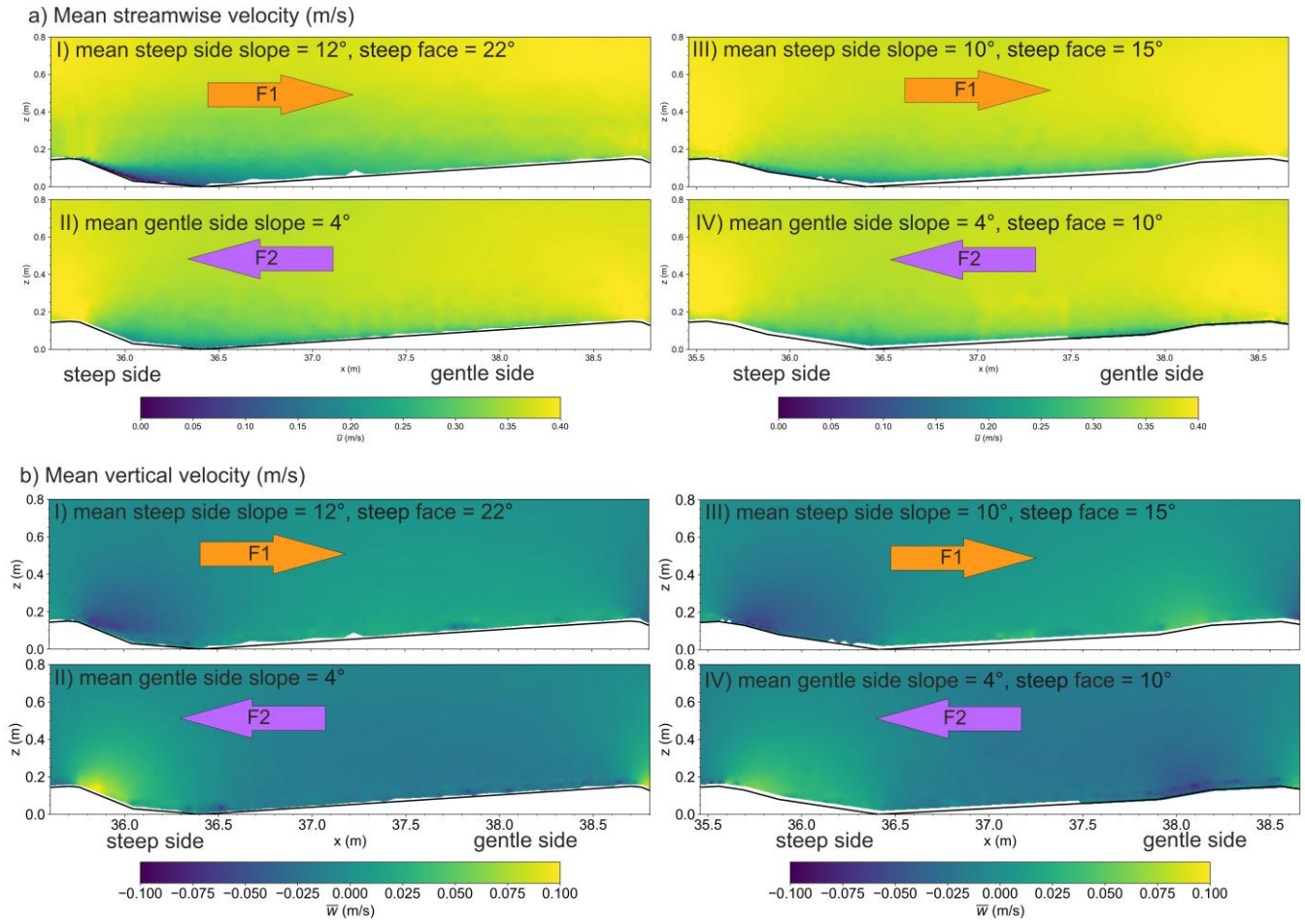

Figure 8. Time-averaged flow fields. I) DUNE1_F1, II) DUNE1_F2, III) DUNE2_F1, IV) DUNE2_F2.

A permanent flow separation zone can be observed very close to the dune surface for both dunes over their steep faces, when the flow is directed from the gentle stoss to the steep lee slope (F1 flow) (Fig. 9). Both flow separations start to develop at or shortly after the brink point, which marks the beginning of the steep face, and are extending over the steep lee side of the dune. Although both dunes show the presence of flow separation, their sizes are different. For DUNE1_F1, the flow separation length is L_{FSZ} = 2.3H or 3.0H_{SF}. The maximum thickness is Th_{FSZ} = 0.14H or 0.18H_{SF}. For DUNE2_F1, the flow separation length and thickness are much shorter and thinner than that of DUNE1_F1 with dimensions of L_{FSZ} = 1.25H or 3.74H_{SF} and Th_{FSZ} = 0.06H or 0.17H_{SF}. Note that both dunes have the same bedform height but different steep face heights.

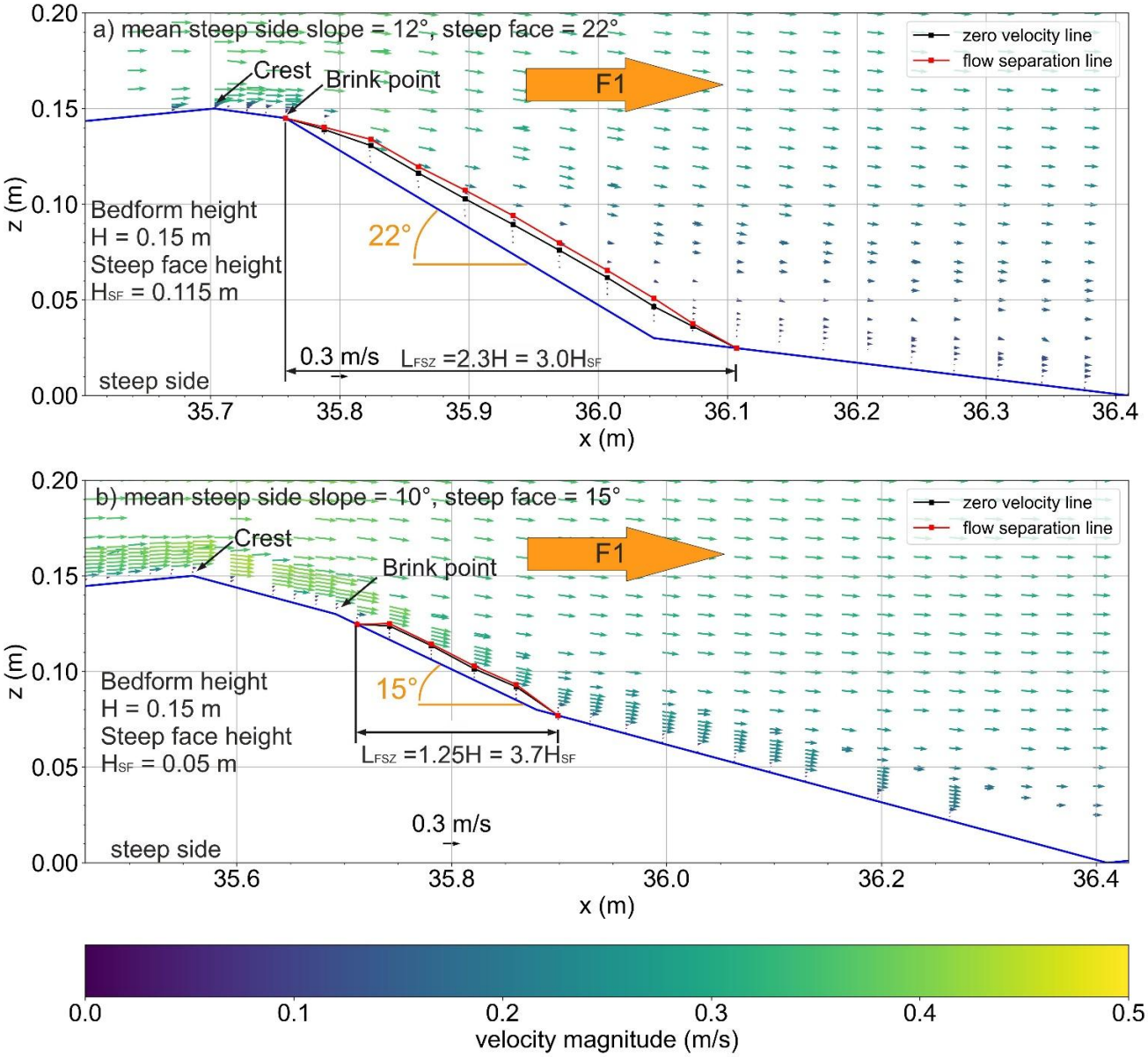

Figure. 9. Permanent flow separation zones. a) DUNE1_F1, b) DUNE2_F1.

310 In order to determine the extents of permanent and intermittent flow separations, the positions of the lines showing the 0% and 50% intermittency factor are calculated (Fig. 10). For DUNE1_F1, an intermittent flow separation extending the entire steep lee side of the dune is detected. Below this intermittent flow separation, a permanent flow separation is limited only to the steep face of the dune. Above DUNE2_F1, the intermittent flow separation becomes almost limited to the steep face and the permanent flow separation is significantly limited in extent compared to DUNE1_F1.

Above DUNE1 and when the flow is directed from the steep stoss to the gentle lee slope (i.e., DUNE1_F2), no permanent flow separation or intermittent flow separation are detected (Fig. 10c). For DUNE2_F2, no permanent flow separation is detected over the gentle lee side of the dune. Interestingly, a small intermittent flow separation is detected over the short steep section (ca. x = 38 – 38.5 m), which has a slope 10°.

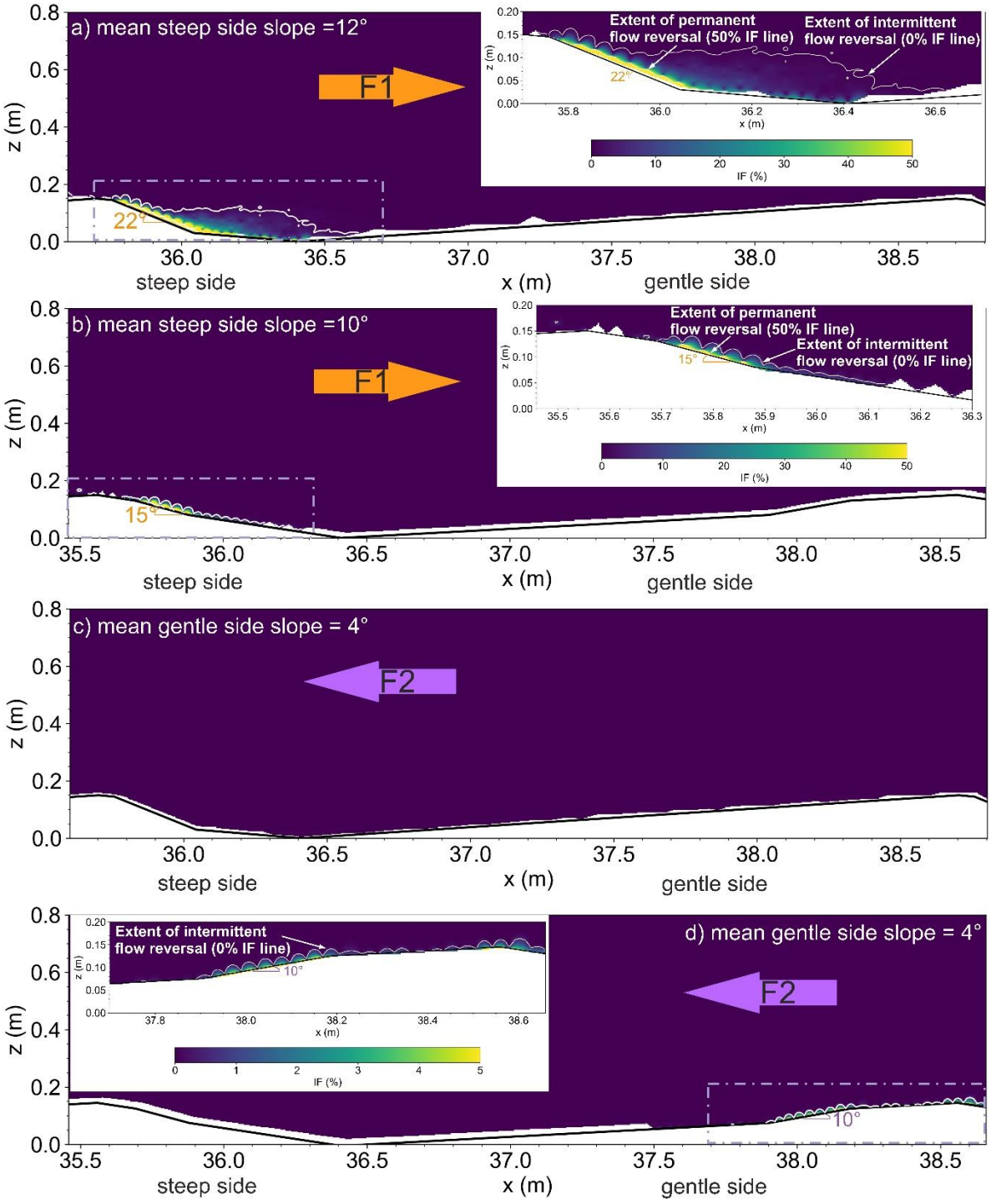

320 **Figure 10. Intermittency factor, IF (%). a) DUNE1_F1, b) DUNE2_F1, c) DUNE1_F2, d) DUNE2_F2. Note different scale used for Fig. 10d.**

Over DUNE1 and when the flow is directed from the gentle stoss to the steep lee slope (i.e., DUNE1_F1), a large and wide horizontal velocity gradient, $\partial\overline{u}/\partial z$, is observed to develop past the brink point and dissipate downstream of the steep lee side and over the gentle stoss side of the next dune (Fig. 11a). The thickest portion of the velocity gradient can be found at the steep face (ca. x = 36.0 m). This steep velocity gradient indicates the presence of a shear layer and significant vorticity. For DUNE2_F1, a thin shear layer, almost attached to the bed and with a diffused-like structure, is observed (Fig. 11b).

Over DUNE1 and when the flow is now directed from the steep stoss to the gentle lee slope (i.e., DUNE1_F2), a very thin and weak shear layer can be seen to develop very close to the bed (Fig. 11c). For DUNE2_F2, characteristics of an attached shear layer similar to that of DUNE1_F2 but with a slightly steeper velocity gradient within the short steep portion (10° slope) can be detected (ca. x = 38 – 38.5 m) (Fig. 11d).

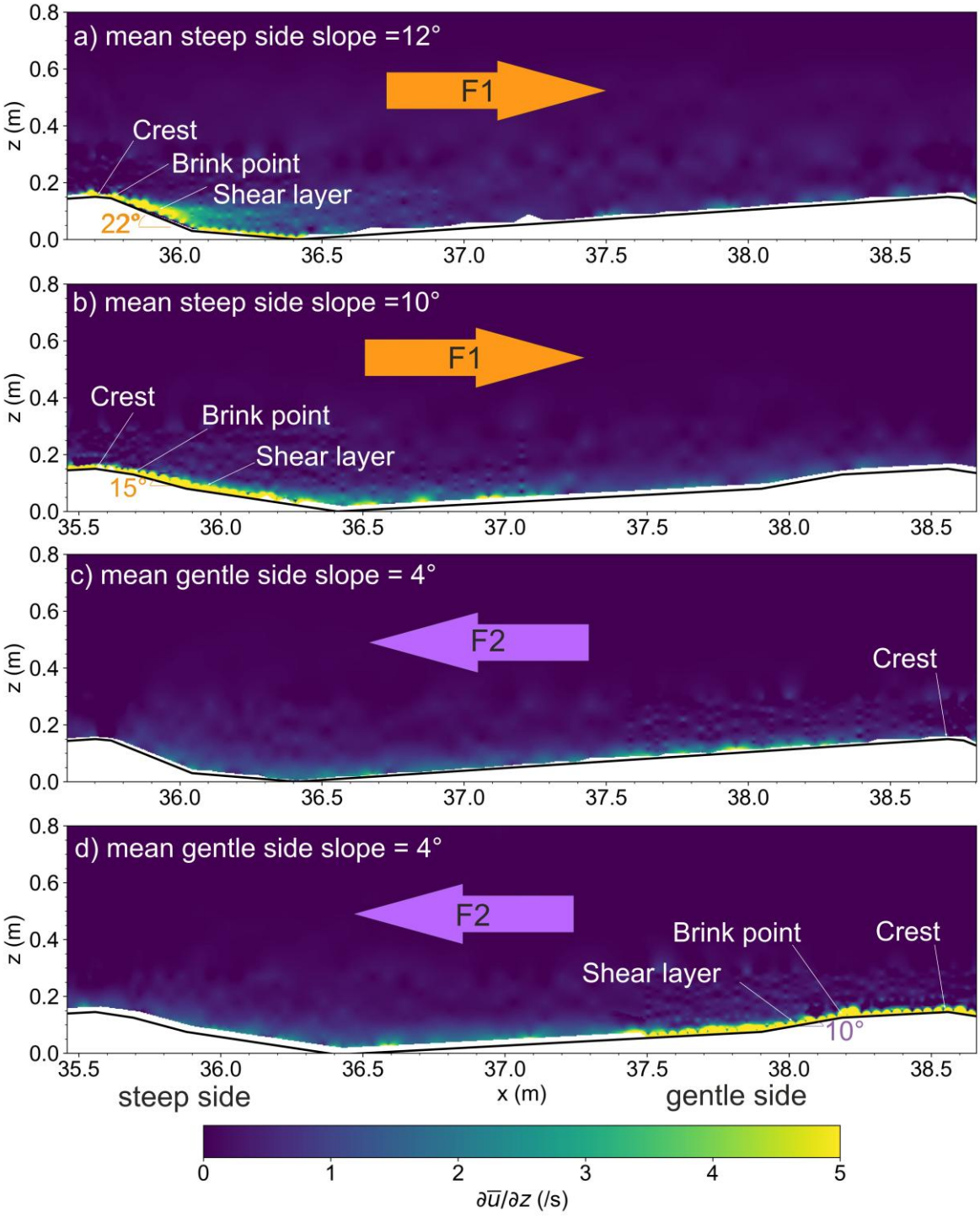

335 **Figure 11. Vertical gradient of time-averaged horizontal velocity, $\partial\overline{u}/\partial z$ (/s). a) DUNE1_F1, b) DUNE2_F1, c) DUNE1_F2, d) DUNE2_F2.**

3.2 Characteristics of turbulence structures over intermediate- and low-angle dunes

For DUNE1_F1, a well-defined turbulent wake can be seen developing just downstream of the brink point above the steep face (Fig. 12a). It propagates downstream of the steep side until it dissipates over the gentle stoss side of the next dune. The strongest portion of the wake with maximum TKE of 0.0089 m^2/s^2 is observed immediately downstream of the steep face (ca. x = 36.0 – 36.1 m). For DUNE2_F1, the turbulence is further reduced with no defined wake structure and a more diffuse pattern can be detected (Fig. 12b). High TKE is concentrated within the immediate vicinity of the bed and diminishes towards the upper portion of the water column. Although not as strong as that of DUNE1_F1, high TKE occurs within the trough and the immediate downstream portion of the gentle stoss side.

When the flow is now directed from the steep stoss to the gentle lee slope of the dune (F2 flow), a similar trend of TKE is observed for both dunes, DUNE1_F2 and DUNE2_F2 (Figs. 12c & d). High TKE is concentrated in the near-bottom region of the flow with no appreciable wake structure. The TKE in the near-bottom flow region diminishes further when there is no steep face present at all (Fig. 11c). Interestingly for DUNE2_F2 (Fig. 12d), a slightly elevated TKE can be detected within the short steep portion (ca. x = 38 – 38.5 m) of the gentle lee slope of the dune but the extent is still limited in the very near-bottom region of the flow.

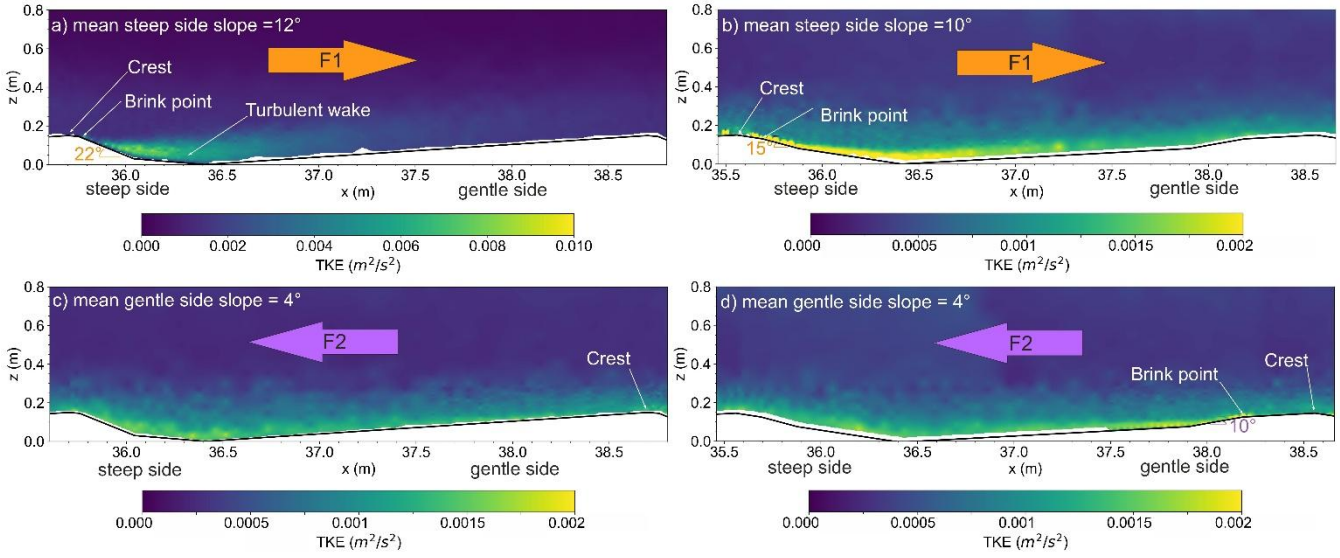

Figure 12. Turbulent kinetic energy, TKE (m^2/s^2). a) DUNE1_F1, b) DUNE2_F1, c) DUNE1_F2, d) DUNE2_F2. Note different scale used for Fig. 12a.

For the four configurations tested in this study, the spatially-averaged Reynolds stresses, $<\tau_{uw}>$, generally increase towards the bed with rapid increase starting from the crest level and then decreases from the zero mean bed elevation down to the dune trough (Fig. 13). The spatially-averaged Reynolds stresses are high when the flow is directed from the gentle stoss to the steep

lee slope (F1 flow, Figs. 13a & c). For DUNE1_F1, the maximum $<\tau_{uw}>$ is about 1.6 Pa at around z = -0.2 m. This means that the spatially-averaged turbulent stresses are high just below mid-height of the dune. For DUNE2_F1, the maximum $<\tau_{uw}>$ is reduced to about 0.6 Pa located near the trough (z = -0.4 m). This still imply that strong turbulent stresses are still occurring within the lower half of the dune height.

When the flow is directed from the steep stoss to the gentle lee slope (F2 flow), the spatially-averaged Reynolds stress profiles for both dunes have an almost comparable vertical structure (Figs. 13b & d). Flow reversal (i.e., F2 flow) reduces significantly the $<\tau_{uw}>$ magnitudes for both dunes. For DUNE1_F2, the maximum $<\tau_{uw}>$ is reduced to about 0.2 Pa almost at the zero mean bed elevation. This still implies that strong turbulent stresses are still occurring around the dune mid-height. Similarly, for DUNE2_F2, the maximum $<\tau_{uw}>$ is also 0.2 Pa just above the zero mean bed elevation.

The spatially-averaged Reynolds stress profile can also provide a direct estimate of the total bottom shear stress as pointed out in previous studies (Nelson et al., 1993; Bennett and Best, 1995; Nikora et al., 2001; Mclean et al., 2008; Kwoll et al., 2016) by performing a regression analysis through the linear segment of the profile and projecting it downwards towards the zero mean bed elevation. The bed shear stress estimation shows a high coefficient of determination for all the linear fits (Fig. 13). For DUNE1_F1, the linear fit is done above z = 0.2 m and from this linear fit, the estimated total bottom shear stress, $\tau_{o,}$ is 0.38 Pa. For DUNE2_F1, the linear fit is above z = 0.34 m with estimated τ_o of 0.06 Pa.

When the flow is reversed and the flow is directed from the steep stoss to the gentle lee slope, a significant reduction in τ_o is observed. Both DUNE1_F2 and DUNE2_F2 yield a τ_o estimate of 0.04 Pa.

These findings show that flow bidirectionality can contribute to significant reduction of turbulence stresses regardless of the dune morphology.

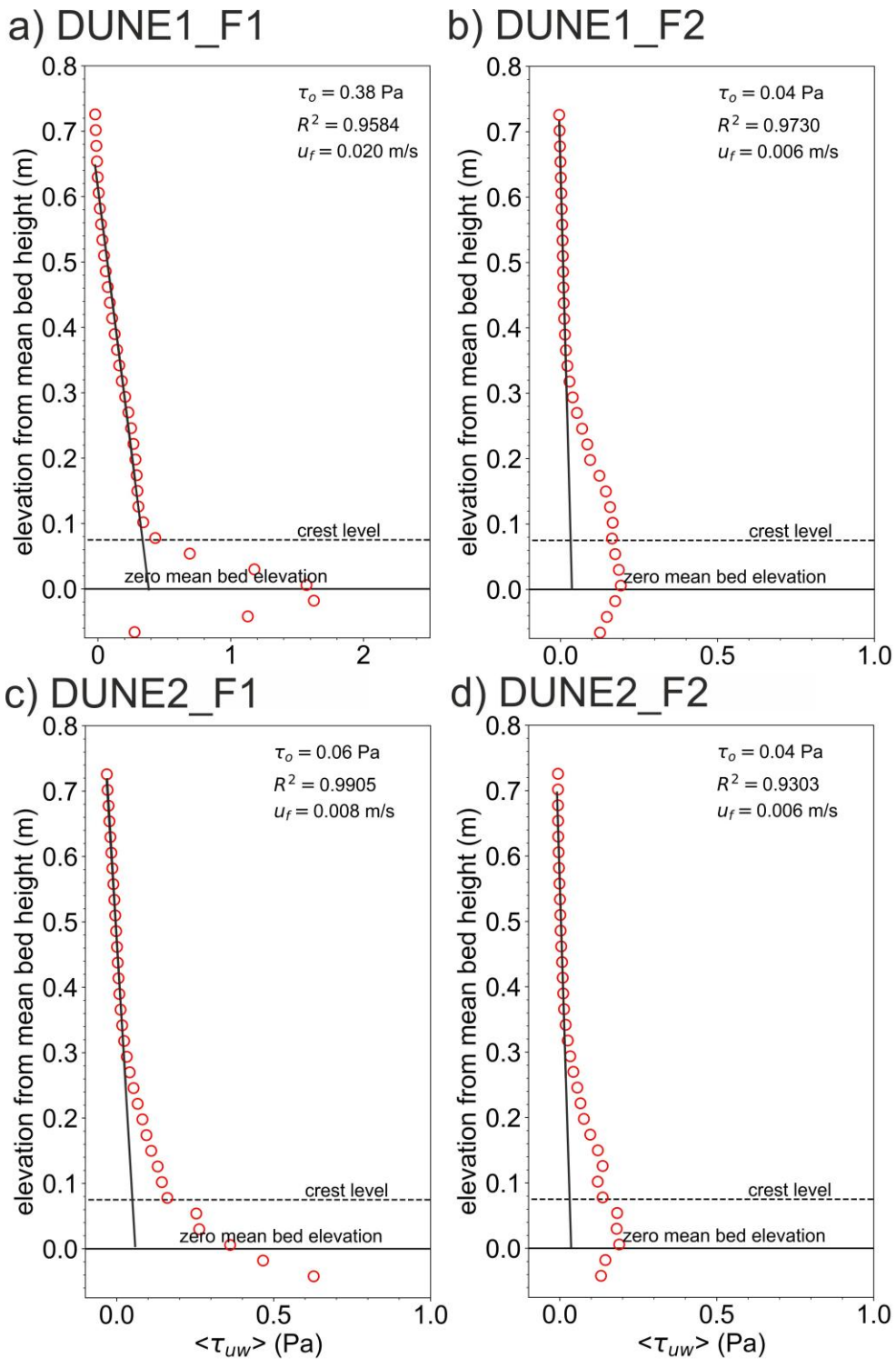

Figure 13. Spatially-averaged Reynolds stress profiles, <τ_{uw}> (Pa). Note different scale for Fig. 13a.

3.3 Characteristics of turbulent events (quadrant analysis)

The results of the quadrant analysis (Fig. 14) depict the percentages of observations for the four quadrant events. Quadrant 1 (Q1, outward interaction) events are fast water burst that moves upward and quadrant 3 (Q3, wallward, inward interaction) events are those slow water bursts that move downward. Both quadrants 1 and 3 are considered negative contributors to Reynolds stresses meaning that they contribute energy to the mean flow by extracting energy from turbulence such as shear layer vortices and coherent flow structures. Quadrant 2 (Q2, ejection) events are low-momentum near-bed fluid being thrown-up into the flow and quadrant 4 (Q4, sweep events) are those high-momentum fluid from above sweeping down into the flow. Both quadrants 2 and 4 are considered positive contributors to Reynolds stresses. Conversely, these turbulent events extract energy from the mean flow contributing to turbulence production.

For the four configurations tested in this study, percentages of observations for outward interaction (Q1) and wallward interaction (Q3) events show an increasing trend above the bed. Elevated percentages for these two events occur within z = 0.4-0.8 m above the bed for both dunes under both flow conditions (F1 and F2). On the other hand, percentages of observations for ejection (Q2) and sweep (Q4) events are highest near the bed and mid water column, especially for ejection events, and decrease toward the surface. Among the four quadrant events, the highest percentage of observations are observed mostly for ejection (Q2) events. High sweep (Q4) occurrences mainly take place in the very near-bottom flow region. These observations are common for both dunes under the two flow directions considered.

Some salient features specific to each dune and flow direction are also observed. For DUNE1_F1, a very intense and high occurrence of ejection (Q2) events are detected at the steep face of the dune and are being brought up further into the water column toward the water surface. These high Q2 occurrences ejected from the steep face are merging to a broader region of high Q2 occurrence located within z = 0.3-0.7 m from the bed. For DUNE2_F1, the same pattern seems to occur also although it is not as pronounced as the previous dune.

When the flow is directed from the steep stoss to the gentle lee slope (F2 flow), the spatial distribution of high ejection (Q2) occurrences changes for both dunes (i.e., DUNE1_F2 and DUNE2_F2). High Q2 occurrences are observed concentrating at the mid-water column around z = 0.2-0.4 m above the bed. Furthermore, high sweep (Q4) occurrences are also observed diminishing at the very near bottom for both dunes when the flow direction changes.

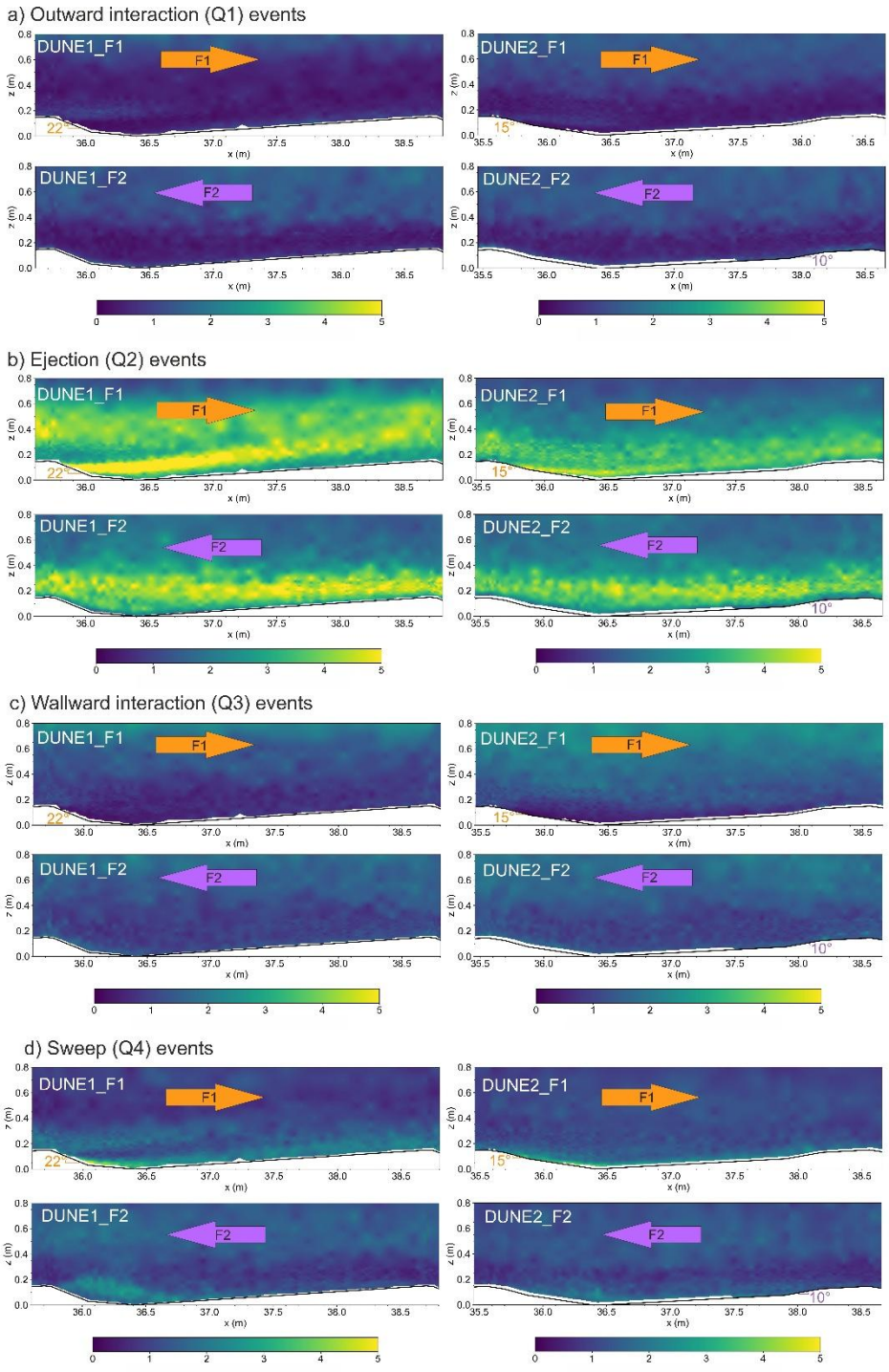

Figure 14. Percentage of observation at each significant quadrant event (%), HS = 2.0. a) Outward interaction event, Q1, b) Ejection event, Q2, c) Wallward interaction event, Q3, d) Sweep event, Q4.

4 Discussion

4.1 Schematic representation of flow and turbulence structures above intermediate- and low-angle tidal dunes

The conceptual diagram presented here demonstrates the significance of flow bidirectionality and dune morphology as controlling factors on the emergence of flow separation, detached shear layer and large-scale turbulence structure over low to intermediate-angle tidal dunes (Fig. 15). Our conceptual diagram emphasises that the same dune morphology can operate in two distinct dynamical regimes depending whether the flow is directed from the gentle stoss to the steep lee slope (as exemplified by our F1 flow) or directed from the steep stoss to the gentle lee slope (as exemplified by our F2 flow) which is a key feature of a bidirectional tidal flows.

Over the intermediate-angle tidal dune and when the flow is directed from the gentle stoss to the steep lee slope (DUNE1_F1), a clear partitioning of the flow structure and turbulence organisation is observed. A permanent flow separation is depicted as largely sweep-dominated (Q4 events) region near the bed while the overlying intermittent flow separation and turbulent wake region contain the more frequent and energetic ejections (Q2 events) that can rise upward and merge with other energetic structures advected from upstream dunes. This streamwise merging of highly energetic regions further support previous observations that influence of upstream bedforms can organise turbulence downstream, rather than individual dune behaving independently.

Over the low-angle dune still under F1 flow (DUNE2_F1), the same directional dependency of flow structures is maintained but the flow separation zones (permanent and intermittent flow separation) and energetic regions become damped. The permanent flow separation shrinks, the intermittent flow separation is narrow and the turbulence signature is weak with the energetic ejection and sweep regions become restricted within the lower water column. With these findings from the two tested dune configurations, we demonstrate that dune morphology modulates the strength and extent of flow and turbulence structures.

The pronounced influence of flow directionality is evident when the flow is reversed and is directed from the steep stoss to the gentle lee slope of the dune (F2 flow). The directional dependency of the steep lee slope implies that the effective lee side becomes gentle (4°). In those cases, our observations show that there is any permanent flow separation but a small intermittent flow separation with a limited extent when a locally steep portion (10°) of the gentle slope is present (DUNE2_F2). Regions of steep velocity gradients and elevated turbulence are observed to be concentrated in the near-bottom region of the flow, consistent with a damped, attached shear layer. Correspondingly, the quadrant activity is weaker and less organised, with reduced presence of both ejection and sweep events relative to F1 flow.

Overall, our conceptual diagram highlights the influence of flow reversal compared to dune geometry that is especially relevant for large tidal dunes. When the flow is directed from the gentle stoss to the steep (low to intermediate-angle) lee slope, an active shear layer and a permanent flow separation develop that can sustain strong, vertically extensive large-scale turbulence structures. When the flow is reversed and is directed from the steep stoss to the gentle (low-angle) lee slope, there is no permanent flow separation, and the turbulent flow structure is shifted towards the bed with an attached shear layer and localised velocity gradients, suppressing the development of large-scale turbulent events.

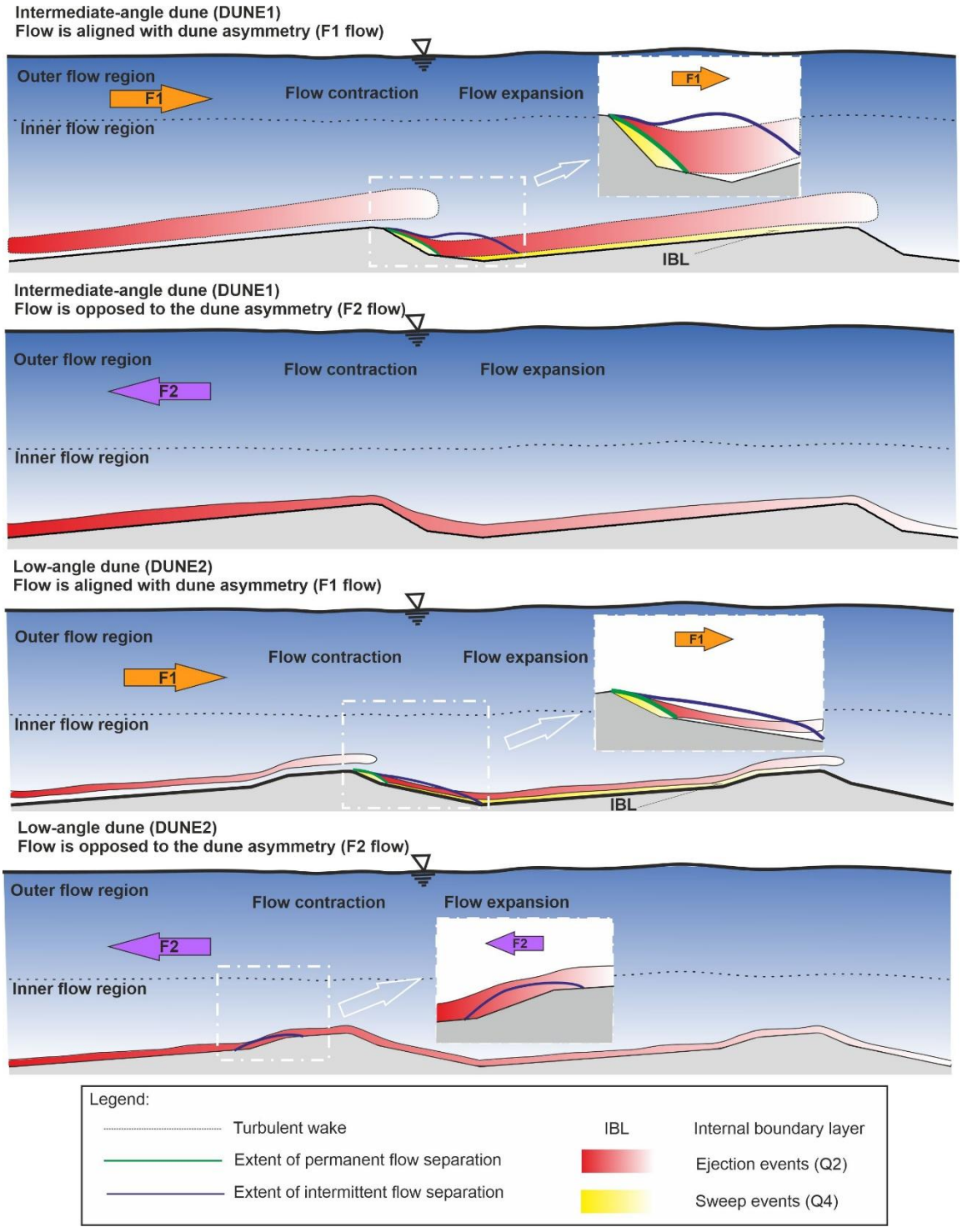

455

Figure 15. Conceptual diagram of flow and turbulence dynamics over intermediate- and low-angle tidal dunes.

4.2 Flow separation zone

Previous studies have pointed out the absence of permanent flow separation over low-angle dunes (Smith and Mclean, 1977; Kostaschuk and Villard, 1996; Roden, 1998; Carling et al., 2000; Best and Kostaschuk, 2002) and the possible presence of intermittent flow separation (Carling et al., 2000; Best and Kostaschuk, 2002). The present findings demonstrate that both permanent flow separation and intermittent flow separation can exist for both intermediate and low-angle dunes depending on the lee side morphology, in particular the presence of a steep slope. This is the case when the flow is directed from the gentle stoss to the steep lee slope of the dune (F1 flow).

While permanent flow separation is well documented over steep asymmetric high-angle dunes (Nelson et al., 1993; Bennett and Best, 1995; Roden, 1998; Kwoll et al., 2016), the permanent flow separation detected in this study especially for the intermediate-angle dune when the flow is directed from the gentle stoss to the steep lee slope (DUNE1_F1) shows contrasting characteristics with typical large permanent flow separation (Best, 2005; Venditti, 2013; Lefebvre et al., 2014a, 2016). The observed permanent flow separation is more elongated and limited in extent. This small permanent flow separation only occupies the near-bottom flow region very close to the bed. Similar to previous observations above high-angle dunes (Bennett and Best, 1995; Kostaschuk, 2000), a small region at the steep face characterised by upward vertical velocity can also be detected. Because of the limited extent of the permanent flow separation above intermediate- and low-angle dunes when the flow is directed from the gentle stoss to the steep lee slope (DUNE1_F1 and DUNE2_F1), the flow separation lengths are much shorter compared to previously reported values typically between 4-6H for high-angle dunes (Engel, 1981; Paarlberg et al., 2007; Lefebvre et al., 2014; Naqshband et al., 2014) , 4.3H-6.5H_{SF} for estuarine dunes (Carstensen and Holzwarth, 2023), 2.1-4.1H for 2D river dunes (Kwoll, 2013; Kwoll et al., 2016) and 5H_{SF} for 3D river dunes (Lefebvre, 2019). The difference in the lengths of permanent flow separation can be attributed to the properties of the steep face (i.e., location and slope angle) as pointed out in previous studies (Lefebvre et al., 2016; Lefebvre, 2019; Lefebvre and Cisneros, 2023). The presence of a steep face is a controlling factor on the generation of flow separation. Over a steep slope such as the case when the flow is directed from the gentle stoss to the steep lee slope, a stronger adverse pressure gradient (i.e., $\partial p/\partial x >> 0$) is encountered by the mean flow leading to a stronger and larger flow expansion which cause a permanent boundary layer separation. Such a process is also pointed out in a previous study about high and low-angle river dunes (Kwoll et al., 2016). On the contrary, only a weaker adverse pressure gradient is encountered over the gentle side of the dune which is not enough to form a permanent flow separation. This is especially true when the flow is directed from the steep stoss to the gentle lee slope (F2 flow).

The intermittent flow separations that have been observed in this study have not been covered in much detail in previous studies. Specifically, we are able to show the presence and extent of intermittent flow separation for intermediate- and low-angle dunes. This study also confirms the previous claim that over low-angle dunes, an intermittent flow separation is present (Carling et al., 2000; Best and Kostaschuk, 2002) regardless of whether a permanent flow separation exists. Furthermore, our

results demonstrate that even for low-angle dune possessing a very gentle mean slope but with some steeper portion, an intermittent flow separation can form. This is the case when the flow is directed from the steep stoss to the gentle lee slope of the dune (DUNE2_F2).

This study provides insights into the influence of flow bidirectionality on the flow and turbulence dynamics above dunes, particularly over intermediate- and low-angle tidal dunes. Flow bidirectionality effectively switches the flow dynamics between a more separated flow regime (F1 flow) and an attached near-bed flow regime (F2 flow) implying that flow separation metrics such as flow separation intermittency and size do not solely depend on morphology but also on flow orientation relative to the dune asymmetry. In the field, this can imply that flow separation may depend strongly on the phase of the tidal cycle and the instantaneous flow separation metrics may not be generalised across the entire tide cycle. Furthermore, field implications highlight that bedforms and their associated flow and turbulence structures respond to changing forcing and can exhibit spatial and temporal variability, consistent with separation regimes that switch with flow reversal.

4.3 Turbulent wake

There are no universally accepted criteria in defining the turbulent wake. For instance, Lefebvre and Cisneros (2023) defined the turbulent wake as the zone where the TKE is twice the mean TKE observed over a flatbed configuration with same flow conditions (i.e., flow velocity and water depth). Studies have also defined the turbulent wake based on a threshold value such as the TKE that is at least 70% of the maximum TKE (Lefebvre et al., 2014a; Lefebvre et al., 2014b; Carstensen and Holzwarth, 2023). Other studies have also defined the turbulent wake as the region characterised by high frequency of ejection (Q2) and sweep (Q4) events (Unsworth et al., 2018). Some have also related the formation of a turbulent wake with the shear layer, pointing out that the turbulent wake is the result of the advected free shear layer which finally diffuses downstream carrying high turbulence intensities, Reynolds stresses and creating a wake structure that is similar to that of wake past a cylinder (Mclean et al., 1994; Bennett and Best, 1995). While most of the above-mentioned literature has used the TKE distribution to define the turbulent wake, the streamwise turbulence intensity (I_u) and Reynolds stress have been also used to define the wake. Specifically, the isolines of I_u = 1.25 and TKE = 2 Pa are said to be a good indicator of defining the turbulent wake (Venditti, 2007).

In this study, we adopt the definition of Lefebvre et al. (2014a) that the turbulent wake is the region enclosed by the isoline of 70% of the maximum TKE and once the wake has been delineated, the extent of the wake is defined as the horizontal distance between the farthest ends of this wake. Since there can be an isolated isoline that passes the threshold, we further restrict our determination of the wake length to consider only the largest contiguous isoline in the TKE distribution. Based on this definition and with a maximum TKE of 0.0089 m^2/s^2 for DUNE1_F1, the turbulent wake extent, L_{wake}, is estimated to be 2.4H or 3.13H_{SF} (Fig. 16). This turbulent wake is smaller compared to, for instance, 5.5H_{SF} (Carstensen and Holzwarth, 2023), 10-17H (Maddux et al., 2003) and 13 H_{SF} (Lefebvre, 2019). This suggests that tidal dunes tend to have shorter wake lengths than river dunes owing to their lower mean slopes and gentler steep face.

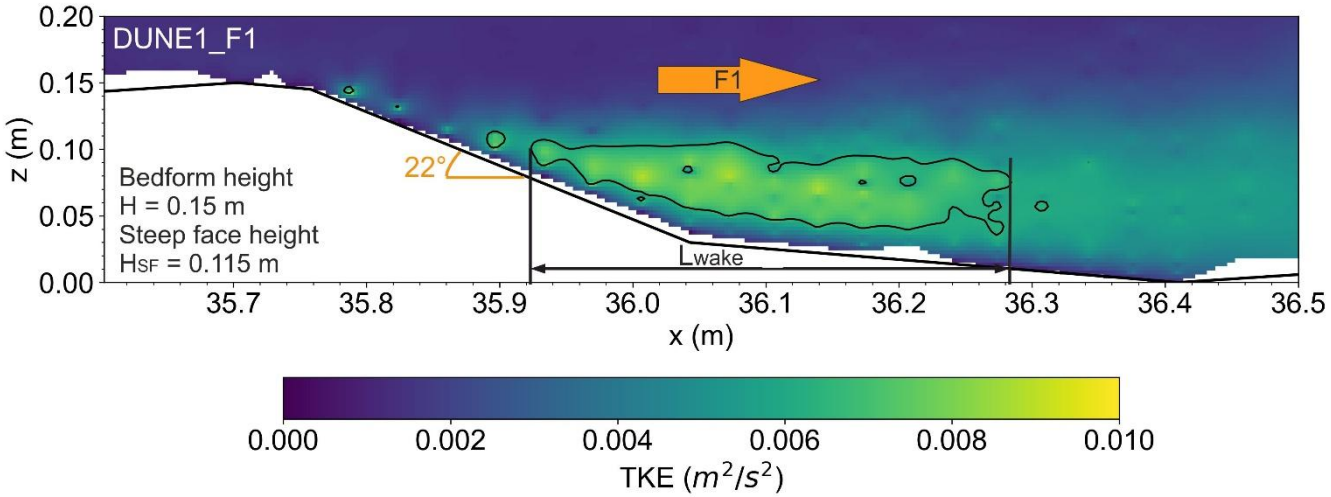

Figure 16. Turbulent wake (70%TKE_{max} isolines) over DUNE1_F1.

In contrast to previous studies where the turbulent wake has been observed to be located high above the dune surface (Best, 2005; Venditti, 2013; Lefebvre et al., 2014a; Lefebvre et al., 2014b; Carstensen and Holzwarth, 2023), the turbulent wake detected in this study is very close to the bed and looks almost attached to it. This is because the shear layer is also very close to the bottom. This finding confirms the intricate relation between the shear layer and the turbulent wake. The observed turbulent wake is also weaker in magnitude compared to that over high-angle dunes (Lefebvre et al., 2014a; Kwoll et al., 2016).

Although there is no appreciable turbulent wake for the other cases with very gentle lee side slopes (F2 flow, when the flow is directed from the steep stoss to the gentle lee slope) on the basis of the 70% TKE_{max} isoline, the overall distribution of the TKE seems to follow a near-wall wake structure similar to that over flatbed conditions (Kline et al., 1967). Similar with flow separation zone, flow bidirectionality again has considerable influence on the presence or absence of a turbulent wake. When the flow is directed from the steep stoss to the gentle lee slope, the turbulence structure transitions into a diffused, near-wall dominated TKE with no appreciable wake structure because the shear layer development is weak and largely attached to the bed. Our findings imply that in the field, turbulent wake formation is likely to be tide phase-dependent, with enhanced wake activity when the flow is directed from the gentle stoss to the steep lee slope (represented by our F1 flow) and markedly reduced when the flow directed from the steep stoss to the gentle lee slope (represented by our F2 flow). Moreover, this phase dependency of wake structure can have further implication on the vertical mixing and suspension of sediments in natural flows (Kwoll et al., 2014).

4.4 Presence and generation of large-scale turbulence structure above intermediate- and low-angle tidal dunes

The quadrant analysis results demonstrate that most of the observed large-scale turbulence structures result from the highly energetic and frequent ejection (Q2) and sweep (Q4) events. Specifically, ejection (Q2) events are dominant in the shear layer

and turbulent wake regions. Sweep (Q4) events are mostly confined in the near-bottom flow especially in the trough section and in the newly formed internal boundary layer. The considerable presence of these turbulent events demonstrates the capability of intermediate- and low-angle dunes to generate large-scale turbulence structures (Kostaschuk and Church, 1993; Best and Kostaschuk, 2002) although their intensity and frequency are weak compared to that over high-angle dunes (Nelson et al., 1993; Bennett and Best, 1995). These findings also imply that the presence of large-scale turbulence might be attributed to intermittent flow separation and does not entirely depend on the presence of permanent flow separation (Best and Kostaschuk, 2002).

Our results suggest that these large-scale turbulences are generated through the shedding of the Kelvin-Helmholtz instabilities along the shear layer (Bennett and Best, 1995; Kadota and Nezu, 1999). This is especially pronounced from the spatial distribution of ejection (Q2) events for both dunes when the flow is directed from the gentle stoss to the steep lee slope (F1 flow) although this is weaker and less intense for the case of low-angle dune. The absence of permanent flow separation while there is still a presence of large-scale turbulence suggests that these structures can be generated if there is a sufficient velocity gradient capable of developing a strong shear layer (Best and Kostaschuk, 2002).

Moreover, flow bidirectionality can also exert considerable influence on the organisation and strength of large-scale turbulence structures. Shear layer development and turbulence production that promote spatially coherent, large-scale turbulence structures are mostly pronounced over intermediate-angle dune and when the flow is directed from the gentle stoss to the steep lee slope. These features are, however, effectively damped when the flow is directed from the steep stoss to the gentle lee slope with the strongest suppression for the case of low-angle dune. This directionally-dependent modulation, similar to that happening for flow separation and turbulent wake, demonstrates that, depending on flow direction, a dune can switch between a macroturbulence-active regime (when the flow goes from the gentle to the steep side, as in our F1 flow conditions) and a largely attached, weakly coherent structure (when the flow goes from the steep to the gentle side, as in our F2 flow conditions), highlighting the importance of accounting for flow reversal in the flow dynamics over tidal dunes. .

The observed large-scale turbulence might also suggest some impact on energy exchange and sediment transport even for the case of intermediate- and low-angle dunes. Ejection (Q2) and sweep (Q4) events feed energy into these turbulence structures by extracting energy from the mean flow via positive contributions to the Reynolds stress (Bennett and Best, 1995; Best and Kostaschuk, 2002; Unsworth et al., 2018). A positive Reynolds stress together with the velocity gradient are the key components for turbulence production. This can also imply that the energy exchange between mean flow and turbulence above low-angle dunes is still enough to generate large-scale turbulence structures. The positive contribution of ejection and sweep events on turbulence has an influence on sediment transport as pointed out in previous studies (Kostaschuk and Church, 1993; Unsworth et al., 2018). For instance, some studies have found out that the upwelling motion of slower fluid particles from the near-bottom flow region caused by the highly frequent significant ejection (Q2) events present in the shear layer and turbulent wake regions

are responsible for the observed elevated suspended sediment concentration on both the crest and lee side of the dune (Thorne et al., 1989; Kostaschuk and Church, 1993; De Lange et al., 2025). On the other hand, the presence of frequent in-rush velocity directed towards the bottom is said to be more responsible for the mobilisation of the more coarser sedimentary materials (i.e., bedload transport) (Thorne et al., 1989).

4.5 Further implications on hydraulic roughness, superimposed dunes and tidal flows

Hydraulic roughness is an important parameter needed to quantify bed shear stress which in turn is needed for estimation of sediment transport. Our observations on flow separation and turbulence dynamics have implications on the effective hydraulic roughness arising from low to intermediate-angle dunes. The estimated total bottom shear stress shown in this study, which can also serve as a proxy for form roughness, is an order of magnitude larger over the intermediate-angle dune than the low-angle dune under the same flow condition (i.e., F1 flow). This sharp reduction in the total bottom shear stress for low-angle dune demonstrates how a lack of flow separation and strong turbulent wake translate to lower form drag and, thus, lowering the effective hydraulic roughness.

Our results can also have important implications for parameterisations of hydraulic roughness in tidal environments. Our findings show that even low-angle dunes (such as our DUNE2, with a gentle side of 4°), a flow separation and turbulence can still be generated suggesting that previous hydraulic roughness estimators based solely on dune height or shape may not be adequate. For example, de Lange et al. (2021) observed that dune size alone accounted for only one third of the variance in hydraulic roughness in the river Waal. They attributed the remaining variance in roughness to multi-kilometer depth variations and other anthropogenic impacts such as groyne structures. These findings point out the need for roughness parameterisations to account not only for dune size but also other topographic and anthropogenic impacts. For dunes that are found in natural tidal environments, the detailed shape of the dune and other hydrodynamic factors such flow reversals and flow directions should be taken into account in roughness estimations (Herrling et al., 2021).

Our tested dune configurations consist only of one scale of dune made of straight lines, and no superimposed secondary dunes were considered. Superimposed dunes, which are small bedforms that ride on the primary dunes, would likely modulate the flow separation and turbulence structures and alter the sediment transport dynamics above intermediate-angle and low-angle tidal dunes. Previous studies have shown how the steepness of the primary dune lee side controls the presence of secondary dunes over the lee side of the primary dune (Zomer et al., 2021). For our intermediate-angle dune when the flow is directed from the gentle stoss to the steep lee slope (DUNE1_F1), superimposed dunes cannot propagate further downstream owing to the steeper lee slope making the flow separation above the primary dune unaltered. For our low-angle dune under the same F1 flow (DUNE2_F1), the gentle lee slope (10°) allows the secondary dunes to propagate over the lee side which might break up the flow expansion zone and can suppress the already small flow separation forming above the primary dune (Dalrymple and Rhodes, 1995; Prokocki et al., 2022). From these two speculations on our tested dunes, it is clear that presence of secondary bedforms can effectively modify the primary dune effective lee side slope. Furthermore, these secondary dunes can also introduce their own micro-scale flow separation and turbulence which may collectively increase the total roughness

(Zomer and Hoitink, 2024; Liu et al., 2025). Overall, the presence of superimposed dunes would induce additional form roughness and can either attenuate or enhance the primary dune flow separation and turbulence structures. This, in turn, would also influence turbulence and sediment flux over the primary dunes (Zomer and Hoitink, 2024).

Another key consideration in natural tidal flows is that they are unsteady, increasing and decreasing during each tidal phase. This unsteadiness may modulate our observed flow and turbulence structures within the tidal cycle. In natural tidal flows, the continually changing flow velocity and direction mean that flow separation and turbulence structure do not have much time to establish a fully developed steady state. Although our flow condition in the experiment is strictly steady unidirectional in two opposite directions which is an idealisation of the real tidal dynamics, we have effectively provided, at a particular time in the tidal cycle, an instantaneous snapshot of the flow and turbulence structures above our intermediate- and low-angle dunes which can serve as a guidance or reference for interpretation of the flow dynamics over natural tidal dunes under realistic tidal flows.

Finally, the present findings complement and help refine conclusions from previous field studies of dune and its associated hydraulic roughness. De Lange et al. (2021) showed that conventional dune geometry predictors underpredict the spatial variability of hydraulic roughness in rivers and that their attempt to correlate roughness with dune lee slopes was not satisfactory. Our experimental results suggest that even dunes with modest lee slopes produce flow separation and macroturbulent structures which might not be captured by simple dune geometry roughness predictors. These other factors could be the intermittent features (intermittent flow separation and shear layer fluctuations) and flow phase dependency which might introduce roughness variability that is not apparent from dune morphology alone, explaining why lee slope metrics do not fully relate to roughness in field settings. Our controlled experiments, which use idealised representation of natural tidal dunes, validate previous conceptual framework on distinct regimes of dune morphology in a fluvial-tidal riverine setting (Prokocki et al., 2022), that in the tidal section of the river, dunes are mainly low-angle (ca. 10 - 15° lee slope) and generate only small flow separation with weaker wakes than high-angle dunes.

In summary, integrating our experimental results with field studies on tidal dunes (De Lange et al., 2021; Prokocki et al., 2022; De Lange et al., 2024) underscores that even intermediate to low angle dunes can still exert considerable impact to flow resistance. Their associated flow separation, if any, and turbulence characteristics must be accounted for to accurately predict hydraulic roughness and sedimental transport under realistic, unsteady tidal flow conditions.

5 Concluding remarks

High-resolution, large-scale flow measurements were conducted over representative intermediate- to low-angle tidal dunes to provide detailed descriptions of the time-averaged flow properties and turbulence structures under bidirectional steady flows. The following conclusions can be drawn from this study:

1. Permanent and intermittent flow separation zones exist for the two tested dune configurations. The properties of the flow separation are directly influenced by the presence and slope of the steep face and mean lee side angle. Specifically, we are able to quantify in detail the shape and extent of both permanent and intermittent flow separations for both intermediate- and low-angle dunes.

2. Over the intermediate-angle dune, the elongated permanent flow separation is short and thin (14% of the flow depth). These characteristics are in contrast with the large and wide permanent flow separation observed for high-angle dunes. An intermittent flow separation that scales with the dune height and covers a wide extent is observed above the small permanent flow separation.

3. Over the low-angle dune, both permanent and intermittent flow separations are detected although their shape and extent are considerably reduced in comparison to the intermediate-angle dune configuration.

4. A distinct turbulent wake is generated above the intermediate-angle dune. The turbulent wake is almost attached to the bed and expands downward before dissipating further over the downstream dune. The wake length is found to be shorter than that of high-angle dunes.

5. No defined wake structure is observed over the tested low-angle dune. Instead, high TKE is concentrated in the very near-bottom region of the flow with a structure similar to a diffuse pattern observed over flatbed conditions.

6. Quadrant analysis results demonstrate the occurrence of large-scale turbulence even for intermediate- and low-angle dunes through the presence of strong and frequent ejection and sweep events. Identification and accounting for large-scale turbulence structure in sediment transport are important as they act as principal drivers of sediment suspension and vertical mixing processes found in natural flow environments.

7. Flow bidirectionality alters the flow and turbulence dynamics for both tested dunes. There is no permanent flow separation for both dunes when the flow is opposed to the dune asymmetry. Interestingly, even if the flow is going over a very gentle slope (4°), an intermittent flow separation can still form provided a small steep (10°) segment is present. Also, a defined turbulent wake does not form for both dunes when the flow direction changes.

8. Finally, our study highlights the capability of intermediate- and low-angle dunes to generate permanent flow separation in contrast to previous claims that it is nonexistent for these types of dunes. Moreover, the results also show that large-scale turbulence is present even in the absence of a permanent flow separation. This implies that a sufficient velocity gradient capable of developing an energetic shear layer is indeed enough to generate large-scale turbulence structures.

Acknowledgements

The authors acknowledge the valuable support of Lars Tretau of BAW Hamburg during the testing, setup and dune installation for the flume experiments in this study. Alexander Alfano of the Faculty of Geoscience, University of Bremen and MARUM is also acknowledged for proofreading the original draft. We sincerely thank Sjoukje de Lange and an anonymous reviewer, as well as the associate editor Anne Baar, who provided constructive comments on the manuscript. We are appreciative of the open access and open review system of Earth Surface Dynamics.

Author contributions

Kevin Bobiles: Conceptualization, Data curation, Methodology, Validation, Investigation, Visualization, Formal analysis, Writing – original draft, Writing – review & editing
Bernhard Kondziella: Methodology, Validation, Investigation, Writing – review & editing
Christina Carstensen: Methodology, Validation, Investigation, Writing – review & editing
Ingrid Holzwarth: Conceptualization, Investigation, Writing – review & editing
Elda Miramontes: Investigation, Writing – review & editing
Alice Lefebvre: Conceptualization, Supervision, Methodology, Investigation, Writing – review & editing, Funding acquisition

Data availability

The experimental data in this study is available at PANGAEA data repository through the link: https://doi.pangaea.de/10.1594/PANGAEA.988194

Competing interests

There are no competing interests among the authors.

Disclaimer

Any opinions, findings and conclusions or recommendations expressed in this material are those of the author(s) and do not necessarily express the views of the institutions to where they belong.

Financial support

Kevin Bobiles has been funded for this study through the German Research Foundation (DFG) project FlowDEB 47010786.

Review statement

References

Aliotta, S. and Perillo, G. M. E.: *A sand wave field in the entrance to Bahia Blanca Estuary, Argentina*, Mar. Geol., 76, 1-14, 10.1016/0025-3227(87)90013-2, 1987.

Bennett, S. J. and Best, J. L.: *Mean flow and turbulence structure over fixed, two-dimensional dunes: implications for sediment transport and bedform stability*, Sedimentology, 42, 491-513, 10.1111/j.1365-3091.1995.tb00386.x, 1995.

Best, J.: *The fluid dynamics of river dunes: A review and some future research directions*, J. Geophys. Res., 110, 21, 10.1029/2004JF000218, 2005.

Best, J. and Kostaschuk, R.: *An experimental study of turbulent flow over a low-angle dune*, J. Geophys. Res., 107, 3135, 10.1029/2000JC000294, 2002.

Bradley, R. W. and Venditti, J. G.: *Reevaluating dune scaling relations*, Earth-Science Reviews, 165, 356-376, 10.1016/j.earscirev.2016.11.004, 2017.

Bradley, R. W., Venditti, J. G., Kostaschuk, R., Church, M. A., Hendershot, M., and Allison, M. A.: *Flow and sediment suspension events over low-angle dunes: Fraser Estuary, Canada*, J. Geophys. Res., 118, 1693-1709, 10.1002/jgrf.20118, 2013.

Carling, P. A., Golz, E., Orr, H. G., and Radecki-Pawlik, A.: *The morphodynamics of fluvial sand dunes in the River Rhine, near Mainz, Germany. I. Sedimentology and morphology*, Sedimentology, 47, 227-252, 10.1046/j.1365-3091.2000.00290.x, 2000.

Carstensen, C. and Holzwarth, I.: *Flow and Turbulence over an Estuarine Dune - Large-Scale Flume Experiments*, Die Küste, 93, 17, https://doi.org/10.18171/1.093103, 2023.

Cisneros, J., Best, J., van Dijk, T., de Almeida, R. P., Amsler, M., Boldt, J., Freitas, B., Galeazzi, C., Huizinga, R., Iannіruberto, M., Ma, H. B., Nittrouer, J. A., Oberg, K., Orfeo, O., Parsons, D., Szupiany, R., Wang, P., and Zhang, Y. F.: *Dunes in the world's big rivers are characterized by low-angle lee-side slopes and a complex shape*, Nat. Geosci., 13, 156-+, 10.1038/s41561-019-0511-7, 2020.

Coleman, S. E. and Nikora, V. I.: *Fluvial dunes: initiation, characterization, flow structure*, Earth Surf. Processes Landforms, 36, 39-57, 10.1002/esp.2096, 2011.

Dalrymple, R. W. and Rhodes, R. N.: *Chapter 13 Estuarine Dunes and Bars*, in: *Dev. Sedimentol.*, edited by: Perillo, G. M. E., Elsevier, 359-422, 1995.

Damen, J. M., Dijk, T. A. G. P. v., and Hulscher, S. J. M. H.: *Spatially Varying Environmental Properties Controlling Observed Sand Wave Morphology*, Journal of Geophysical Research: Earth Surface, 123, 19, https://doi.org/10.1002/2017JF004322, 2018.

de Lange, S. I., Naqshband, S., and Hoitink, A. J. F.: *Quantifying Hydraulic Roughness From Field Data: Can Dune Morphology Tell the Whole Story?*, Water Resour. Res., 57, e2021WR030329, 10.1029/2021WR030329, 2021.

de Lange, S. I., van de Vijsel, R. C., Torfs, P. J. J. F., Wallerstein, N. P., and Hoitink, A. J. F.: *Bimodality in subaqueous dune height suggests flickering behavior at high flow*, Nature Communications, 16:6317, 9, https://doi.org/10.1038/s41467-025-61248-5, 2025.

de Lange, S. I., Bradley, R., Schrijvershof, R., Murphy, D., Waldschläger, K., Kostaschuk, R., Venditti, J., and Hoitink, A. J. F.: *Dune geomtery and the associated hydraulic roughness in the fluvial to tidal transition zone of the Fraser River at low river flow*, Journal of Geophysical Resarch: Earth Surface, 129, e2023JF007340, 25, https://doi.org/10.1029/2023JF007340, 2024.

Engel, P.: *Length of Flow Separation over Dunes*, J. Hydraul. Div., 107, 1133-1143, 1981.

Goring, D. G. and Nikora, V. I.: *Despiking Acoustic Doppler Velocimeter Data*, J. Hydraul. Eng., 128, 10, 10.1061/~ASCE!0733-9429~2002!128:1~117!, 2002.

Herrling, G., Becker, M., Lefebvre, A., Zorndt, A., Kramer, K., and Winter, C.: *The effect of asymmetric dune roughness on tidal asymmetry in the Weser estuary*, Earth Surf. Processes Landforms, 18, 10.1002/esp.5170, 2021.

Kadota, A. and Nezu, I.: *Three-dimensional structure of space-time correlation on coherent vortices generated behind dune crest*, Journal of Hyraulic Research 37, 22, 1999.

Kline, S. J., Reynolds, W. C., Schraub, F. A., and Runstadler, P. W.: *The structure of turbulent boundary layers*, J. Fluid Mech., 30, 33, 10.1017/S0022112067001740, 1967.

Kostaschuk, R.: *A field study of turbulence and sediment dynamics over subaqueous dunes with flow separation*, Sedimentology, 47, 519-531, 10.1046/j.1365-3091.2000.00303.x, 2000.

Kostaschuk, R. and Church, M. A.: *Macroturbulence generated by dunes: Fraser River, Canada*, Sediment. Geol., 85, 25-37, 10.1016/0037-0738(93)90073-E, 1993.

Kostaschuk, R. and Villard, P.: *Flow and sediment transport over large subaqueous dunes: Fraser River, Canada*, Sedimentology, 43, 849-863, 10.1111/j.1365-3091.1996.tb01506.x, 1996.

Kostaschuk, R., Blair, J., Villard, P., and Best, J.: *Morphological response of estuarine subtidal dunes to flow over a semidiurnal tidal cycle: Fraser River, Canada*, MARID II, Marine and River Dune Dynamics, Enschede, Netherlands, 1-2 April, 160-167,

Kwoll, E.: *Bedforms, macroturbulence, and sediment transport at the fluid-bed interface*, Departement of Geosciences, University of Bremen, 88 pp., 2013.

Kwoll, E., Venditti, J. G., Bradley, R. W., and Winter, C.: *Flow structure and resistance over subaquaeous high- and low-angle dunes*, Journal of Geophysical Research: Earth Surface, 121, 545-564, 10.1002/2015JF003637, 2016.

Kwoll, E., Venditti, J. G., Bradley, R. W., and Winter, C.: *Observations of Coherent Flow Structures Over Subaqueous High- and Low- Angle Dunes*, Journal of Geophysical Research: Earth Surface, n/a-n/a, 10.1002/2017JF004356, 2017.

Lange, D., Müller, H., Piechotta, F., and Schubert, R.: *The Weser Estuary*, Die Küste, 74, 13, 20.500.11970/101611, 2008.

Lefebvre, A.: *Three-Dimensional Flow Above River Bedforms: Insights From Numerical Modeling of a Natural Dune Field (Río Paraná, Argentina)*, Journal of Geophysical Research: Earth Surface, 124, 2241-2264, 10.1029/2018jf004928, 2019.

Lefebvre, A. and Cisneros, J.: *The influence of dune lee side shape on time-averaged velocities and turbulence*, Earth Surf. Dynam., 11, 575-591, 10.5194/esurf-11-575-2023, 2023.

Lefebvre, A., Paarlberg, A. J., and Winter, C.: *Flow separation and shear stress over angle of repose bedforms: a numerical investigation*, Water Resour. Res., 50, 986-1005, 10.1002/2013WR014587, 2014a.

Lefebvre, A., Paarlberg, A. J., and Winter, C.: *Characterising natural bedform morphology and its influence on flow*, Geo-Mar. Lett., 36, 379–393, 10.1007/s00367-016-0455-5, 2016.

Lefebvre, A., Paarlberg, A. J., Ernstsen, V. B., and Winter, C.: *Flow separation and roughness lengths over large bedforms in a tidal environment: a numerical investigation*, Cont. Shelf Res., 91, 57-69, 10.1016/j.csr.2014.09.001, 2014b.

Lefebvre, A., Herrling, G., Becker, M., Zorndt, A., Krämer, K., and Winter, C.: *Morphology of estuarine bedforms, Weser Estuary, Germany*, Earth Surf. Processes Landforms, 10.1002/esp.5243, 2021.

Liu, R., Cheng, H., Chen, J., Teng, L., Ren, Z., Yang, Q., Fan, H., and Lefebvre, A.: *Subaqueous multiscale bedform morphology dynamics in a mountainous macrotidal estuary*, Frontiers in Marine Science, 12:1585285, 20, doi: 10.3389/fmars.2025.1585285, 2025.

Maddux, T. B., Nelson, J. M., and McLean, S. R.: *Turbulent flow over three-dimensional dunes: 1. Free surface and flow response*, Journal of Geophysical Research: Earth Surface, 108, 10.1029/2003JF000017, 2003.

McLean, S. R., Nelson, J. M., and Wolfe, S. R.: *Turbulence structure over two-dimensional bed forms: Implications for sediment transport*, J. Geophys. Res., 99, 12729-12747, 10.1029/94JC00571, 1994.

McLean, S. R., Nikora, V. I., and Coleman, S. E.: *Double-averaged velocity profiles over fixed dune shapes*, Acta Geophys., 56, 2008.

Naqshband, S., Ribberink, J. S., Hurther, D., and Hulscher, S. J. M. H.: *Bed load and suspended load contributions to migrating sand dunes in equilibrium*, J. Geophys. Res., 119, 1043–1063, 10.1002/2013JF003043, 2014.

Nasner, H.: *Prediction of the Height of Tidal Dunes in Estuaries*, in: *Coastal Engineering 1974*, 1036-1050, https://doi.org/10.1061/9780872621138.063, 1974.

Nasner, H., Pieper, R., and Torn, P.: *Dredging of tidal dunes*, Coastal Engineering 2008, 2761-2773, https://doi.org/10.1142/9789814277426_0228, 2009.

Nelson, J. M., McLean, S. R., and Wolfe, S. R.: *Mean flow and turbulence fields over two-dimensional bed forms*, Water Resour. Res., 29, 3935-3953, 10.1029/93WR01932, 1993.

Nikora, V. I., Goring, D., McEwan, I., and Griffiths, G.: *Spatially averaged open-channel flow over rough bed*, J. Hydraul. Eng., 127, 11, 10.1061/(ASCE)0733-9429(2001)127:2(123), 2001.

Nortek: *Nortek: The Comprehensive Manual for Velocimeters. Vector, Vectrino, Vectrino Profiler*, 119, https://support.nortekgroup.com/hc/en-us/articles/360029839351-The-Comprehensive-Manual-Velocimeters, 2018.

Paarlberg, A. J., Dohmen-Janssen, C. M., Hulscher, S. J. M. H., and Termes, P.: *A parameterization of flow separation over subaqueous dunes*, Water Resour. Res., 43, W12417, 10.1029/2006WR005425, 2007.

Porcile, G., Mouazé, D., Weill, P., Gangloff, A., and Bennis, A.-C.: *PIV Measurements of Turbulent Water Flows Over Fixed Low-Angle Compound Dunes Under Reversing Currents* Journal of Geophysical Research: Oceans, 130, 25, https://doi.org/10.1029/2025JC022418, 2025.

Prokocki, E. W., Best, J. L., Perillo, M. M., Ashworth, P. J., Parsons, D. R., Sambrook Smith, G. H., Nicholas, A. P., and Simpson, C. J.: *The morphology of fluvial-tidal dunes: Lower Columbia River, Oregon/Washington, USA*, Earth Surf. Processes Landforms, 47, 2079-2106, 10.1002/esp.5364, 2022.

Roden, J. E.: *The sedimentology and dynamics of mega-dunes, Jamuna River, Bangladesh*, Ph.D., Department of Earth Sciences, University of Leeds, Leeds, UK, 310 pp., 1998.

Smith, J. D. and McLean, S. R.: *Spatially averaged flow over a wavy surface*, J. Geophys. Res., 84, 1735-1746, 10.1029/JC082i012p01735, 1977.

Sukhodolov, A., Fedele, J., and Rhoads, B. L.: *Structure of flow over alluvial bedforms: an experiment on linking field and laboratory methods*, Earth Surf. Processes Landforms, 31, 19, 10.1002/esp.1330, 2006.

Thorne, P. D., Williams, J. J., and Heathershaw, A. D.: *In situ acoustic measurements of marine gravel threshold and entrainment*, Sedimentology, 36, 14, 1989.

Unsworth, C. A., Parsons, D. R., Hardy, R. J., Reesink, A. J. H., Best, J. L., Ashworth, P. J., and Keevil, G. M.: *The Impact of Nonequilibrium Flow on the Structure of Turbulence Over River Dunes*, Water Resour. Res., 54, 6566-6584, 10.1029/2017WR021377, 2018.

Venditti, J. G.: *Turbulent flow and drag over fixed two- and three-dimensional dunes*, J. Geophys. Res., 112, F04008, 10.1029/2006JF000650, 2007.

Venditti, J. G.: *Bedforms in sand-bedded rivers*, in: *Treatise on Geomorphology*, edited by: Shroder, J., and Wohl, E., Academic Press, San Diego, CA, 137-162, 10.1016/B978-0-12-374739-6.00235-9, 2013.

Venditti, J. G. and Bennett, S. J.: *Spectral analysis of turbulent flow and suspended sediment transport over fixed dunes*, J. Geophys. Res., 105, 22035-22047, 10.1029/2000JC900094, 2000.

Venditti, J. G., Church, M., and Bennett, S. J.: *Morphodynamics of small-scale superimposed sand waves over migrating dune bed forms*, Water Resour. Res., 41, 10.1029/2004WR003461, 2005.

Villard, P. and Kostaschuk, R.: *The relation between shear velocity and suspended sediment concentration over dunes: Fraser Estuary, Canada*, Mar. Geol., 148, 71-81, 10.1016/S0025-3227(98)00015-2, 1998.

Zomer, J. Y. and Hoitink, A. J. F.: *Evidence of Secondary Bedform Controls on River Dune Migration* Geophys. Res. Lett., 51, e2024GL109320, 9, https://doi.org/10.1029/2024GL109320, 2024.

Zomer, J. Y., Naqshband, S., Vermeulen, B., and Hoitink, A. J. F.: *Rapidly Migrating Secondary Bedforms Can Persist on the Lee of Slowly Migrating Primary River Dunes*, Journal of Geophysical Research: Earth Surface, 126, e2020JF005918, doi.org/10.1029/2020JF005918, 2021.